Linear control and estimation of nonlinear chaotic convection: Harnessing the butterfly effect

Thomas R. Bewley[a]
Center for Turbulence Research, Stanford University, Stanford, California 94305

This paper examines the application of linear optimal/robust control theory to a low-order nonlinear chaotic convection problem. Linear control feedback is found to be fully effective only when it is switched off while the state is far from the desired equilibrium point, relying on the attractor of the system to bring the state into a neighborhood of the equilibrium point before control is applied. Linear estimator feedback is found to be fully effective only when (a) the Lyapunov exponent of the state estimation error is negative, indicating that the state estimate converges to the uncontrolled state, and (b) the estimator is stable in the vicinity of the desired equilibrium point. The aim in studying the present problem is to understand better some possible pitfalls of applying linear feedback to nonlinear systems in a low-dimensional framework. Such an exercise foreshadows problems likely to be encountered when applying linear feedback to infinite-dimensional nonlinear systems such as turbulence. It is important to understand these problems and the remedies available in a low-dimensional framework before moving to more complex systems. © *1999 American Institute of Physics.* [S1070-6631(99)01105-8]

I. AIM AND SCOPE

The high sensitivity of nonlinear chaotic systems, such as fluid convection and turbulence, to small levels of external forcing may be exploited to stabilize such systems with small levels of coordinated feedback. It is demonstrated in this paper that linear state feedback is capable of regulating a nonlinear convection problem from an arbitrary initial fluid state by modulation of the rate of heating applied to the system. It is similarly demonstrated that a nonlinear estimator with linear measurement feedback is capable of estimating the nonlinear convection problem based on measurements of the lateral temperature fluctuations in the fluid. As we will show, special care must be taken in both cases, as the nonlinearity of the system has important consequences. Finally, a state estimator and a controller may be combined to regulate the present nonlinear convection problem to the desired flow state based on limited state measurements.

The aptness of linear state feedback for regulating the nonlinear convection system with full state information is first characterized. An important difficulty with the direct application of linear feedback to the nonlinear problem is identified: specifically, an aggravated undesired flow state is stabilized by the linear feedback in addition to the desired flow state, and the domain of convergence to this undesired state is large. Further, closed-loop system response when strong linearly stabilizing control is applied may even be unbounded, although the desired flow state is endowed with a high degree of linear stability. An effective solution to this problem is demonstrated: namely, the convection system

may be ''caught'' with a linearly stabilizing controller by applying control only when the state is ''near'' the desired state, relying on the chaotic dynamics of the uncontrolled system to bring the state into such a neighborhood before control is applied.

The aptness of nonlinear estimators forced with linear measurement feedback for estimating the nonlinear convection system with limited noisy measurements is then characterized. The nonlinearity makes the estimation problem fundamentally different than the control problem: more than just linear stability of infinitesimal estimation errors at a single location in phase space is required to build an estimator which is effective for the uncontrolled nonlinear system. However, convergence of the estimator is possible with direct linear feedback when appropriate feedback gains are used even though the estimator so constructed is not stable over the entire attractor of the uncontrolled system. The nature of the estimation problem is examined, weak conditions for effective estimator behavior (based on the Lyapunov exponent of the estimation error) are established, and an effective state estimator is determined.

Finally, conclusions are drawn and related questions are raised about the implications of the present work on the application of linear control theory to the infinite-dimensional nonlinear problem of turbulence.

II. BACKGROUND

A. Nominal behavior of the convection system

By major simplification of a buoyancy-driven flow problem governed by the Navier–Stokes equation,[1,2] Edward Lorenz derived and characterized a simple set of ordinary dif-

[a]Current address: Dept. of MAE, UC San Diego, La Jolla, California 92093, phone: (858) 534-4287; fax: (858) 822-3107; electronic mail: bewley@ucsd.edu

(a) Semi-infinite 2D convection rollers.
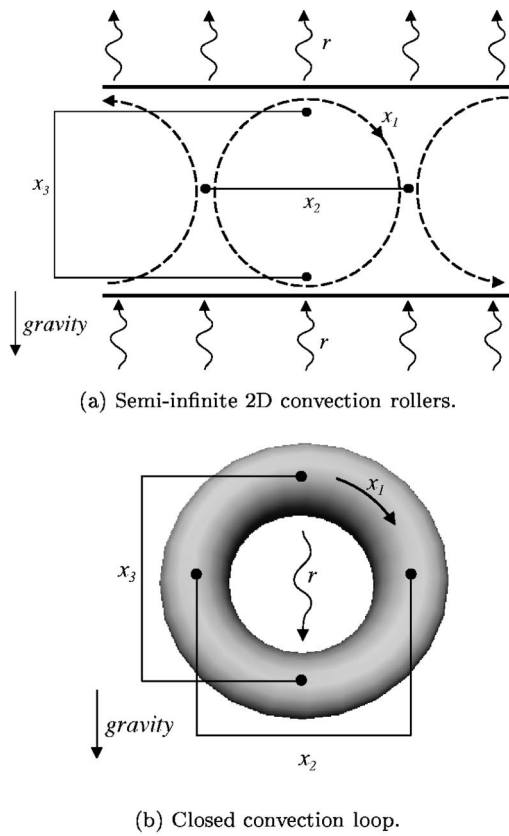

(b) Closed convection loop.

FIG. 1. Geometry of two chaotic convection problems, approximately governed by Eq. (1), to which unsteady heating $r = \bar{u} + u'$ may be applied in order to stabilize a stationary convection state. Only the convection in the torus illustrated in (b), which is restricted by its geometry to a single mode, is accurately governed by Eq. (1) when the steady-state heating rate is sufficiently high ($\bar{u} > r_H$) that the convection phenomenon is chaotic.[7]

ferential equations which models a fluid convection problem (Fig. 1) and exhibits chaotic behavior (Fig. 2). This system may be expressed as

$$\dot{x}_1 = \sigma(x_2 - x_1),$$

$$\dot{x}_2 = -x_2 - x_1 x_3, \quad\quad (1)$$

$$\dot{x}_3 = -bx_3 + x_1 x_2 - br,$$

where x_1 is proportional to the intensity of the fluid motion, x_2 is proportional to the lateral temperature fluctuations in the fluid, and x_3 is proportional to the vertical temperature fluctuations in the fluid. The loop Rayleigh number r is proportional to the heating rate at the bottom of the convective system, the loop Prandtl number σ is related to the fluid's kinematic viscosity and thermal conductivity, the quantity b is related to the fluid's thermal expansion coefficient, and all variables have been nondimensionalized.[1] Lorenz showed that fluid motion in this system is chaotic for a sufficiently high rate of heating $r > r_H = \sigma(\sigma + b + 3)/(\sigma - b - 1)$. In this paper, all computations are carried out for parameter values typical for a laboratory-scale implementation[3] of the geometry of Fig. 1(b) in the chaotic regime, nominally, $\sigma = 4$, $b = 1$, and $r = 3r_H = 48$.

The Lorenz equation was originally derived as a low-order model of the semi-infinite convection phenomenon illustrated in Fig. 1(a), roughly modeling the solar heating at the bottom of a layer of convection cells in the earth's atmosphere.[1,2] However, the Lorenz equation models accurately only simple roll convection for $r < r_H$, when the steady two-dimensional convection rollers are stable.[4] Chaotic motion in this system is characterized by the interaction of several Fourier modes, and thus is not adequately modeled by Eq. (1).

As shown by Yorke and Yorke[5] and Gorman, Widmann, and Robins,[6,7] a confined toroidal geometry, as illustrated in Fig. 1(b), can prevent other major convection modes from forming. When heated from below and cooled at the same rate from above (e.g., with a simple heat pump), this system is approximately governed by Eq. (1) well into the chaotic regime $r > r_H$. Its simple geometry and construction makes this model system a prime candidate for the study of the feedback control of chaotic fluid phenomena, much as the inverted pendulum has become a standard testbed for the control of unstable systems in dynamics. Both problems represent easily constructed minimum realizations of important unstable phenomena in large-scale systems, and thus a thorough understanding of the estimation and control of these model systems is illuminating.

Note that the present work assumes a laminar drag law in the derivation of the governing equation.[7] Note also that, for implementations in which the heating and cooling rates are not identical (such as the experimental apparatus of Wang, Singer, and Bau[3]), a fourth equation may be incorporated into the system model in order to increase its fidelity by accounting for the fluctuations of the average temperature in the loop.[7,8] System identification techniques may also be used to develop even higher-order ODE models that capture the secondary instabilities of the flow in the torus. Such secondary instabilities are important for large values of r and for geometries in which the minor radius of the torus is not sufficiently small as compared to the major radius.

The chaotic behavior of the uncontrolled system (see Fig. 2) is well understood.[1,4,9,10] Under the present conditions, the trajectory of the state meanders deterministically but nonperiodically around two unstable focus points $\bar{\mathbf{x}}$ and $\bar{\mathbf{x}}'$ and an unstable saddle point $\bar{\mathbf{x}}''$, where, defining $c_1 = \sqrt{b(r-1)}$,

$$\bar{\mathbf{x}} = \begin{pmatrix} c_1 \\ c_1 \\ -1 \end{pmatrix}, \quad \bar{\mathbf{x}}' = \begin{pmatrix} -c_1 \\ -c_1 \\ -1 \end{pmatrix}, \quad \text{and} \quad \bar{\mathbf{x}}'' = \begin{pmatrix} 0 \\ 0 \\ -r \end{pmatrix}.$$

The system takes from one to several cycles around each focus point alternately. The unstable focus $\bar{\mathbf{x}}$ corresponds to uniform clockwise fluid motion, the unstable focus $\bar{\mathbf{x}}'$ corresponds to uniform anti-clockwise fluid motion, and the unstable saddle $\bar{\mathbf{x}}''$ corresponds to zero fluid motion.

Note that Fig. 2(c) illustrates that the sheet containing the attractor is twisted in such a way that the intermittent maxima in x_3 along the state trajectory in the quadrant near either focus point may occur on either of two lobes. This
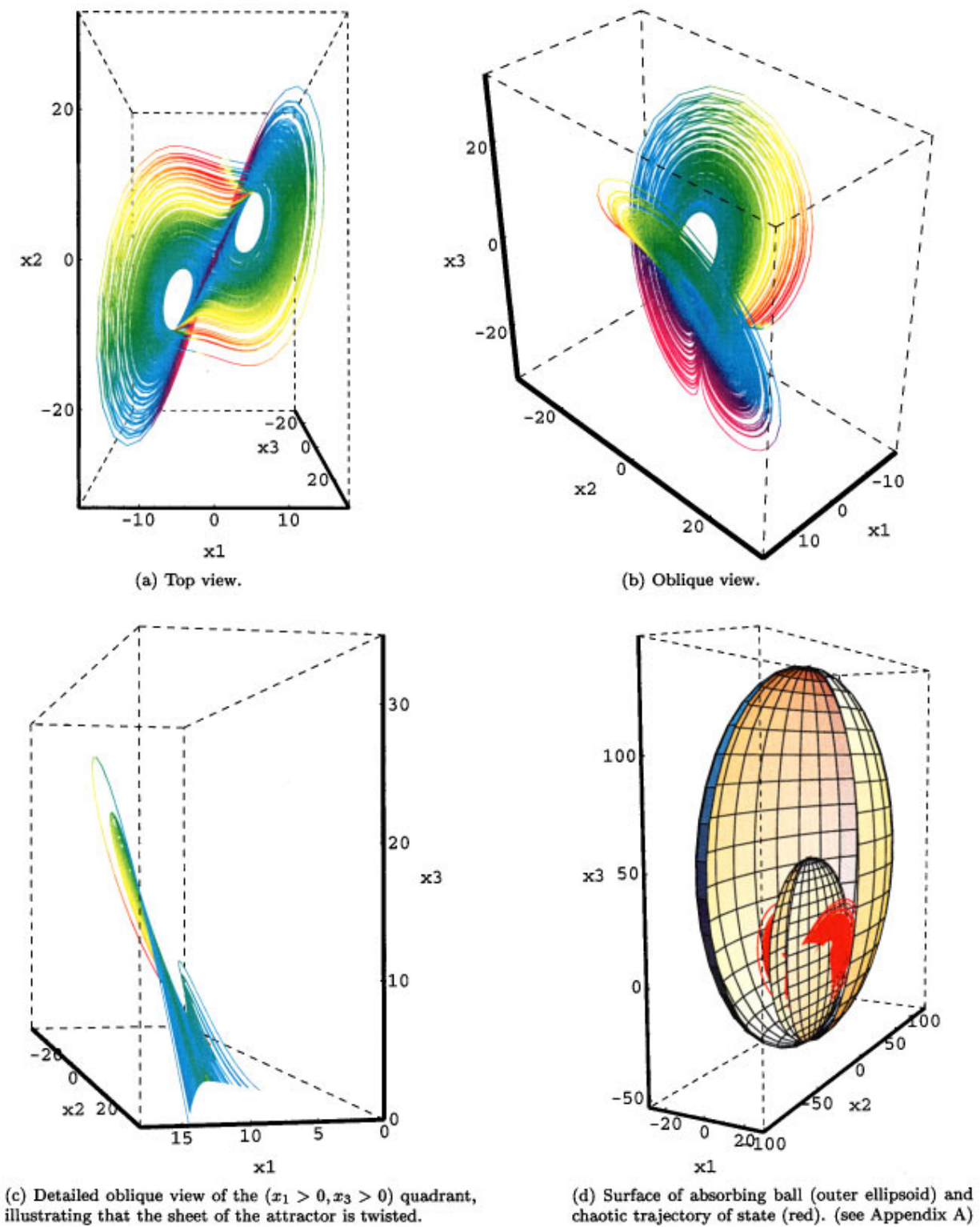
(a) Top view.

(b) Oblique view.

(c) Detailed oblique view of the $(x_1 > 0, x_3 > 0)$ quadrant, illustrating that the sheet of the attractor is twisted.

(d) Surface of absorbing ball (outer ellipsoid) and chaotic trajectory of state (red). (see Appendix A)

FIG. 2. Trajectory of the state **x** in phase space for a convection problem governed by the Lorenz equation with $\sigma=4$, $b=1$, and $r=3r_H=48$. In 2(a)–2(c), violet and blue indicate the portion of the attractor with positive local Lyapunov exponent (Ref. 13) (diverging trajectories) whereas red and yellow indicate the portion of the attractor with negative local Lyapunov exponent (converging trajectories). Other figures characterizing this attractor are available at http://turbulence.ucsd.edu/~bewley/lorenz.

results in the multiple-valued Poincaré map of Fig. 3 (i.e., draw a vertical line and it intersects the curve in at least four places). Note that the smaller of the two lobes is visited very infrequently; over 40 000 peaks in x_3 were computed in order to produce the plot shown in Fig. 3.

The chaotic motion of the present convection system is characterized by trajectories which, when integrated over the attractor, diverge exponentially. The system, therefore, is highly sensitive to small disturbances. Such disturbances may arise from a variety of sources, including:
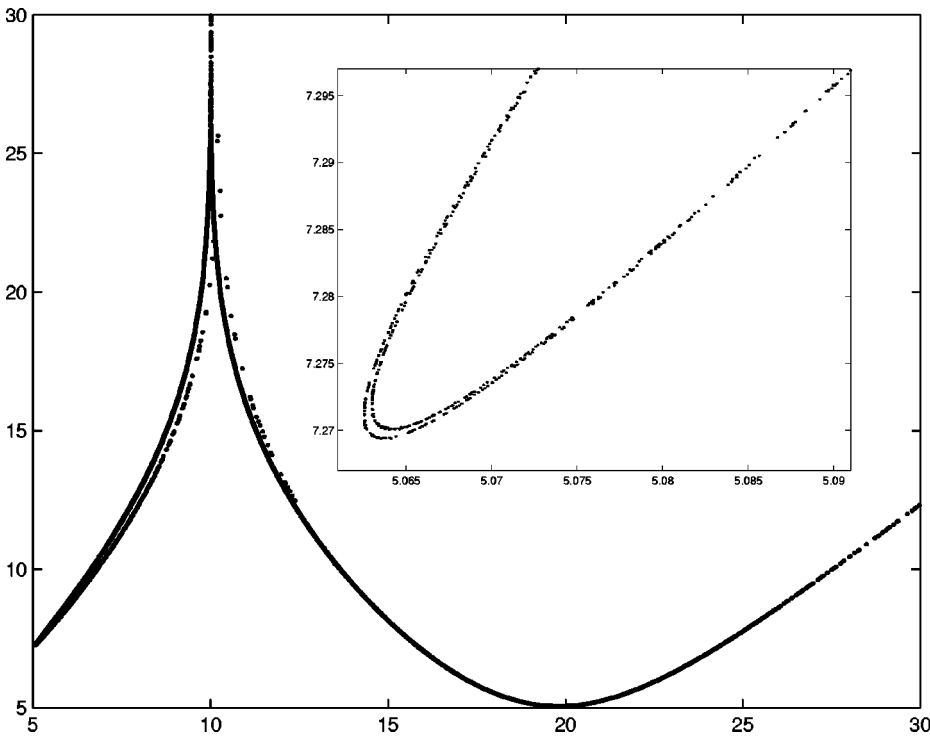
FIG. 3. Poincaré map of the uncontrolled Lorenz system ($\sigma=4$, $b=1$, $\bar{u}=48$, $u'=0$). The jth maximum of $x_3(t)$ is plotted as a function of the ($j-1$)th maximum of $x_3(t)$, a common technique used to characterize the nature of a chaotic system (Ref. 1). Note that the map is multiple valued. Points to the right of each cusp are accompanied by a change in sign of x_1, whereas points to the left of each cusp are accompanied by no change in sign of x_1. Near the lower-left corner of the map, as illustrated in greater detail in the inset, the curvature is smooth (not cusped) and the map is at least quadruple valued.

(a)   modification of the initial conditions,
(b)   unmodeled perturbations to the control applied (in this case taken to be the heating rate), and
(c)   unmodeled perturbations to the governing equation (such as those resulting from secondary flows and other unmodeled system dynamics).

For PDE systems such as turbulence, the sources of disturbance may be identified as perturbations to the initial conditions, the boundary conditions, and the PDE itself. This sensitivity to perturbations is loosely referred to in the popular literature as the ''butterfly effect:'' [4,10,11]

> disturbances of magnitude commensurate with the flap of a butterfly's wing are sufficient to alter substantially the trajectory of the system over a long time interval.

Note that the trajectory from two almost identical initial states may take a long time to diverge, although the exponential divergence of the system will eventually dominate under most circumstances.

The convergence or divergence of system trajectories is made precise by the Lyapunov exponent and the local Lyapunov exponent.[12-14] Consider an infinitesimal perturbation $\delta\mathbf{x}(0)$ of an initial state $\mathbf{x}(0)$. The perturbation $\delta\mathbf{x}(t)$ evolves in the tangent space of $\mathbf{x}(t)$ according to the linearization of Eq. (1), which is given by

$$\dot{\delta x}_1 = \sigma(\delta x_2 - \delta x_1),$$

$$\dot{\delta x}_2 = -\delta x_2 - x_1\delta x_3 - x_3\delta x_1,$$

$$\dot{\delta x}_3 = -b\,\delta x_3 + x_1\delta x_2 + x_2\delta x_1.$$

The Lyapunov exponent λ_∞ is defined as

$$\lambda_\infty = \lim_{T\to\infty} \frac{1}{T}\log\frac{\|\delta\mathbf{x}(T)\|}{\|\delta\mathbf{x}(0)\|}$$

for almost all initial states $\mathbf{x}(0)$ and initial infinitesimal perturbations $\delta\mathbf{x}(0)$. The Lyapunov exponent thus measures the exponential rate of convergence ($\lambda_\infty<0$) or divergence ($\lambda_\infty>0$) of perturbed trajectories of the system when averaged over long time intervals ($T\to\infty$). For the present parameter values, the Lyapunov exponent was calculated to be $\lambda_\infty=0.707$. The local Lyapunov exponent $\lambda_\epsilon(\mathbf{x}(t))$ is defined as

$$\lambda_\epsilon(\mathbf{x}(t)) = \lim_{T\to0} \frac{1}{T}\log\frac{\|\delta\mathbf{x}(t+T)\|}{\|\delta\mathbf{x}(t)\|}$$

for almost all initial states $\mathbf{x}(0)$ and initial infinitesimal perturbations $\delta\mathbf{x}(0)$ and for t sufficiently large that $\mathbf{x}(t)$ lies on the attractor and $\delta\mathbf{x}(t)$ points along the expanding direction in tangent space.[13] The local Lyapunov exponent thus measures the local exponential rate of convergence or divergence of trajectories on the attractor, and the Lyapunov exponent is the long-time average along the system trajectory $\mathbf{x}(t)$ of the local Lyapunov exponent (see Figs. 2 and 4). It is shown in Appendix D that the Lyapunov exponent is a general property of the system in the sense that it is independent of the choice of norm used in its definition, although this is not true of the local Lyapunov exponent. (In our present computations, we take $\|\cdot\|$ to be the Euclidean norm.) These quantities will be extended in Sec. IV to examine the convergence or divergence of the state estimation error when linear feedback is applied.
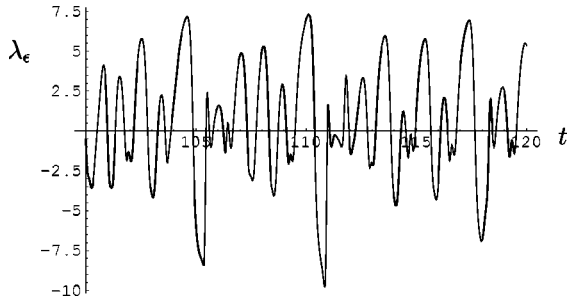
FIG. 4. The local Lyapunov exponent $\lambda_\epsilon(t)$ for the uncontrolled system (as computed with the Euclidean norm) as the state moves on the attractor. The average of the local Lyapunov exponent integrated over the path of the attractor gives the Lyapunov exponent $\lambda_\infty = 0.707$, indicating that perturbed trajectories diverge exponentially.

B. The control problem

Interest in the convection model of Lorenz has been re-kindled recently by attempts to control chaotic phenomena. As shown in this paper, the system sensitivity described above may be harnessed to control the present problem with small amounts of linear feedback.

In the present control problem, a steady-state heating rate $\bar{u}$ is modulated by an unsteady control u' such that

$$r = \bar{u} + u'.$$

The control problem considered here is to find an algorithm for computing the control u' (modulation of the cooling/heating rate at the top/bottom of the apparatus) based on limited observations of the state (specifically, noisy measurements of x_2) in order to stabilize the focus point corresponding to time-invariant clockwise motion of the fluid $\bar{\mathbf{x}}$, which is stationary but linearly unstable in the uncontrolled ($u' = 0$) Lorenz system for $\bar{u} > r_H$. This model control problem, introduced in the linear optimal context by Vincent[15] and Yuen and Bau,[16] has been the topic of several recent investigations.[3,11,15–21] The present study characterizes certain problems which arise when linear feedback is used for the estimation and control of the Lorenz system. These issues should be well understood on this model nonlinear system before applying linear feedback to more complex non-linear systems such as turbulence, as discussed in Sec. VI.

C. State disturbances and measurement noise

State disturbances are inevitable in the present system, and come from sources such as unmodeled heat transfer and secondary flows. Noise of some level in the measurement is also inevitable, and arises from inaccuracies of the thermo-couples measuring the temperature difference x_2 and from the electronics processing their signals, which are often quite low voltage. These "disturbances," as they shall generically be referred to, are now accounted for in a general form; details of the disturbance scaling outlined here, using the same notation as the present development, may be found in Ref. 22.

Define G_1 as the square root of the expected covariance of the state disturbances to be added to the three components of Eq. (1) and α as the rms amplitude of the noise of the

(scalar) temperature measurement. It is assumed that G_1 and α are time invariant. In the present problem, as nothing is known about the state disturbances *a priori*, they are assumed to have the simple covariance $G_1 \triangleq I$. Known structure of the covariance of the state disturbance (for example, knowledge of where the unmodeled heat transfer is likely to occur) is accounted for by replacing $G_1 = I$ with an appropriate matrix of unit maximum singular value, retaining the quantity α to reflect the ratio between the magnitude of the measurement noise and the magnitude of the state disturbance.[22] As any covariance of the disturbances known in advance is accounted for in G_1 and α, the external disturbance vector $\mathbf{w}$ taken to drive this problem is assumed to be, in the optimal case, an uncorrelated, zero-mean, white Gaussian process and, in the robust case, an unstructured disturbance with equal weighting on all states.

The externally disturbed system equation for $\dot{\mathbf{x}}$ and the equation for the noisy flow measurement $\mathbf{y}$ of the left/right temperature difference x_2 are written in matrix form as

$$\dot{\mathbf{x}} = A\mathbf{x} + N(\mathbf{x}) + B_1\mathbf{w} + B_2\mathbf{u} + \mathbf{r}, \tag{2a}$$

$$\mathbf{y} = C_2\mathbf{x} + D_{21}\mathbf{w}, \tag{2b}$$

with

$$\mathbf{x} \triangleq \begin{pmatrix} x_1 \\ x_2 \\ x_3 \end{pmatrix}, \quad \mathbf{u} \triangleq (u'), \quad \mathbf{r} \triangleq \begin{pmatrix} 0 \\ 0 \\ -b\bar{u} \end{pmatrix},$$

$$A \triangleq \begin{pmatrix} -\sigma & \sigma & 0 \\ 0 & -1 & 0 \\ 0 & 0 & -b \end{pmatrix}, \quad N(\mathbf{x}) \triangleq \begin{pmatrix} 0 \\ -x_1 x_3 \\ x_1 x_2 \end{pmatrix},$$

$$B_1 \triangleq (G_1 \quad 0), \quad B_2 \triangleq \begin{pmatrix} 0 \\ 0 \\ -b \end{pmatrix},$$

$$C_2 \triangleq (0 \quad 1 \quad 0), \quad \text{and} \quad D_{21} \triangleq (0 \quad \alpha I).$$

The appropriate transfer function norms, reflecting the response of the closed-loop systems to be developed to small (linear) disturbances $\mathbf{w}$, are tabulated in the following two sections. For clarity, the simulations of the full nonlinear systems in the present work are performed with the disturbance vector $\mathbf{w} = \mathbf{0}$. In this way, we analyze the nonlinear dynamics of the closed-loop systems separately from their small-disturbance response characteristics.

III. DETERMINATION OF AN EFFECTIVE CONTROL STRATEGY

In this section, we present an effective control strategy for the nonlinear system Eq. (2a) when full state information is available for determining the control. Initially, linear optimal/robust control theory is used to compute control feedback which linearly stabilizes the desired state. Subsequently, the resulting (linear) control feedback is applied to the full nonlinear problem, as discussed in the Introduction.

Define the perturbation $\boldsymbol{\xi}$ of the state $\mathbf{x}$ from the desired state $\bar{\mathbf{x}}$ such that

$$\boldsymbol{\xi} \triangleq \mathbf{x} - \bar{\mathbf{x}}.$$

The stabilization of uniform clockwise motion is equivalent to the regulation of the perturbation $\boldsymbol{\xi}$ to zero. We would like

TABLE I. Optimal controller feedback gains ($\gamma=\infty$) and linear disturbance rejection near desired fixed point ($\mathbf{x}=\bar{\mathbf{x}}$). Transfer function norms reported measure the linearized response of the closed-loop system to state disturbances when the system is near the linearization point $\mathbf{x}=\bar{\mathbf{x}}$ for which the controllers were designed. [†]Case studied by Yuen and Bau (Ref. 16).

ℓ	K			$\|T_{\xi\mathbf{w}}\|_2$	$\|T_{\xi\mathbf{w}}\|_\infty$	$\|T_{\mathbf{uw}}\|_2$
1000	(0.3222	-0.3222	1.3277)	1.848	3.173	1.946
10	(0.3247	-0.3254	1.3392)	1.832	3.120	1.946
1 [†]	(0.4696	-0.5424	2.0719)	1.296	1.512	2.083
0.50	(0.6541	-0.9428	3.2341)	0.994	0.847	2.400
0.25	(0.8722	-1.9933	5.6581)	0.774	0.466	2.980
0.10	(0.4843	-6.4708	12.7740)	0.622	0.269	4.128
0.050	(-1.8511	-15.8700	23.8717)	0.575	0.271	5.311
0.025	(-8.1871	-36.3081	44.8130)	0.551	0.273	7.049
0.010	(-29.1673	-99.2058	105.5891)	0.536	0.268	10.759

to accomplish this regulation with a limited amount of control $\mathbf{u}$. In the robust setting, we would even like to accomplish such regulation in the presence of a finite disturbance $\mathbf{w}$ which maximally spoils the control objective. Thus following the approach of standard linear optimal/robust control theory, the problem under consideration is expressed as the *minimization* of a control objective $\mathcal{J}$ with respect to the control $\mathbf{u}$ and the simultaneous *maximization* of the control objective $\mathcal{J}$ with respect to the disturbance $\mathbf{w}$, where

$$\mathcal{J} \triangleq E[\boldsymbol{\xi}^* Q \boldsymbol{\xi} + \ell^2 \mathbf{u}^* \mathbf{u} - \gamma^2 \mathbf{w}^* \mathbf{w}]$$
$$= E[\mathbf{z}^* \mathbf{z} - \gamma^2 \mathbf{w}^* \mathbf{w}],$$

the expectation value $E[\cdot]$ is defined as the long-time-averaged expected value of the quantity in brackets for almost all initial states $\boldsymbol{\xi}(0)$ and (in the optimal case) unit-norm white Gaussian disturbances $\mathbf{w}$, and the performance measure $\mathbf{z}$ is defined such that

$$\mathbf{z} \triangleq C_1 \boldsymbol{\xi} + D_{12} \mathbf{u}, \tag{3}$$

with

$$C_1 \triangleq \begin{pmatrix} Q^{1/2} \\ 0 \end{pmatrix} \quad \text{and} \quad D_{12} \triangleq \begin{pmatrix} 0 \\ \ell I \end{pmatrix}.$$

As all of the elements of the state are similarly scaled, it is reasonable to take $Q=I$. The parameter ℓ^2 denotes the price of the control. Reduced values of ℓ penalize the cost function less upon the application of control, and thereby tend to result in larger control magnitudes, $E[\mathbf{u}^* \mathbf{u}]$, and smaller excursions of the perturbation, $E[\boldsymbol{\xi}^* Q \boldsymbol{\xi}]$. Similarly, the parameter γ^2 denotes the ''price'' of the disturbance, in the spirit of a noncooperative game. Note that setting $\gamma \to \infty$ eliminates the disturbance from the noncooperative game ($\mathbf{w} \to \mathbf{0}$ in the maximization w.r.t. $\mathbf{w}$), resulting in the optimal control result. Reduced values of γ introduce a finite component of the worst-case disturbance to the problem, generally resulting in larger feedback gains targeted at stabilizing the system response to the worst-case disturbance. Further discussion of the nature of this noncooperative game is deferred to Ref. 22.

The equation governing the state perturbation $\boldsymbol{\xi}$ (in fact, for any reference point $\bar{\mathbf{x}}$) is easily derived[1] from Eq. (2a) and written in matrix form as

$$\dot{\boldsymbol{\xi}} = \bar{A} \boldsymbol{\xi} + N(\boldsymbol{\xi}) + B_1 \mathbf{w} + B_2 \mathbf{u} + \bar{\mathbf{r}}, \tag{4}$$

where the linearized system matrix $\bar{A}$ and the constant vector $\bar{\mathbf{r}}$ take the form

$$\bar{A} \triangleq A + \begin{pmatrix} 0 & 0 & 0 \\ -\bar{x}_3 & 0 & -\bar{x}_1 \\ \bar{x}_2 & \bar{x}_1 & 0 \end{pmatrix}, \quad \bar{\mathbf{r}} \triangleq A\bar{\mathbf{x}} + N(\bar{\mathbf{x}}) + \mathbf{r}.$$

Note that $\bar{\mathbf{r}} = \mathbf{0}$ because $\bar{\mathbf{x}}$ is taken here to be a stationary point of the uncontrolled system Eq. (1). For sufficiently small perturbations $\boldsymbol{\xi}$, the nonlinear term $N(\boldsymbol{\xi})$ is small compared with the linear terms. Thus for a state $\mathbf{x}$ in a sufficiently small neighborhood of the desired state $\bar{\mathbf{x}}$, the controller feedback $\mathbf{u}$ solving the noncooperative game discussed above for the nonlinear system Eq. (2a) may be determined by analysis of just the linear terms of Eq. (4).

The linear operator $\bar{A}$ is unstable for $\bar{u} > r_H$. For the present parameter values, the eigenvalues of $\bar{A}$ are $\{-6.66, 0.33 \pm 7.50i\}$. As the complex eigenvalues have positive real parts, a small perturbation to the state $\mathbf{x}$ from the stationary point $\bar{\mathbf{x}}$ causes the state to spiral away from the stationary point in the uncontrolled system.

A linear controller of the form

$$\mathbf{u} = K\boldsymbol{\xi} = K(\mathbf{x} - \bar{\mathbf{x}}) \tag{5a}$$

solving the noncooperative game discussed above for the linearization of the system Eq. (4) governing the state perturbation $\boldsymbol{\xi}$ is given by the controller feedback

$$K = -\frac{1}{\ell^2} B_2^* X, \tag{5b}$$

where

$$X = \text{Ric} \begin{pmatrix} \bar{A} & \frac{1}{\gamma^2} B_1 B_1^* - \frac{1}{\ell^2} B_2 B_2^* \\ -C_1^* C_1 & -\bar{A}^* \end{pmatrix}, \tag{5c}$$

and Ric($\cdot$) denotes the solution of the associated Riccati problem,[23] in accordance with standard linear optimal/robust control theory.[24–26,22] Resulting feedback matrices K for representative ℓ and γ are given in Tables I and II.

Inserting a linear controller of the form $\mathbf{u} = K\boldsymbol{\xi}$ into Eq. (4) and rearranging, the closed-loop system matrix takes the

TABLE II. Robust controller feedback gains ($l=10$) and linear disturbance rejection near desired fixed point (see legend of Table I).

γ	K			$\|T_{\xi\mathbf{w}}\|_2$	$\|T_{\xi\mathbf{w}}\|_\infty$	$\|T_{\mathbf{uw}}\|_2$
∞	(0.3247	-0.3254	1.3392)	1.832	3.118	1.946
25	(0.5151	-0.7188	2.4580)	1.161	1.193	2.189
20	(0.6855	-1.8348	4.7175)	0.832	0.556	2.775
18	(-0.5661	-8.7956	13.0871)	0.619	0.257	4.246
17.5	(-11.2060	-41.0934	39.9697)	0.554	0.248	7.316
17.35	(-128.2235	-365.7229	285.2543)	0.533	0.243	20.442
$\gamma_0 \approx 17.33$	(-3377.5645	-9338.9540	7028.6511)	0.530	0.242	102.676

form $\bar{A}+B_2K$. For the present parameter values with, for example, $\ell=0.25$ and $\gamma=\infty$ and K computed from Eq. (5), the eigenvalues of $\bar{A}+B_2K$ are $\{-6.70, -2.48\pm7.39i\}$. As all eigenvalues now have negative real parts, any small perturbation to the state $\mathbf{x}$ from the stationary point $\bar{\mathbf{x}}$ causes the state to spiral back to the stationary point in the controlled system.

The linear (i.e., small) disturbance rejection of the various controllers K near the desired stationary point $\mathbf{x}\approx\bar{\mathbf{x}}$ is quantified by the appropriate transfer function norms.[27] The precise mathematical description of these transfer function norms is summarized in Ref. 22. In short,

$\|T_{\xi\mathbf{w}}\|_2$ measures the rms value of the state perturbation ξ in response to small white Gaussian disturbances $\mathbf{w}$,

$\|T_{\xi\mathbf{w}}\|_\infty$ measures the rms value of the state perturbation ξ in response to small disturbances $\mathbf{w}$ with the worst-case structure, and

$\|T_{\mathbf{uw}}\|_2$ measures the rms value of the control $\mathbf{u}$ in response to small white Gaussian disturbances $\mathbf{w}$.

As seen in Table I, decreasing the parameter ℓ results in increased control feedback ($\|T_{\mathbf{uw}}\|_2$) to counteract disturbances with stronger control, thereby resulting in a smaller state response to Gaussian disturbances ($\|T_{\xi\mathbf{w}}\|_2$). Decreasing ℓ also happens to reduce the state response to worst-case disturbances ($\|T_{\xi\mathbf{w}}\|_\infty$) fairly effectively.

Table II illustrates the effect of accounting for a finite component of the worst-case disturbance in the control problem by reducing γ. Starting from one of the optimal controllers of Table I (specifically, the one with $\ell=10$), reducing γ effectively reduces the response of the state to worst-case disturbances ($\|T_{\xi\mathbf{w}}\|_\infty$). There is a minimum value $\gamma=\gamma_0$ below which the Riccati equation (5c) cannot be solved. For γ close to this value, the feedback gains are quite large, although such increased feedback has only a small effect on $\|T_{\xi\mathbf{w}}\|_\infty$. Due to the possibility of system uncertainties, actuator saturation, and measurement noise, large feedback gains are not desirable, and intermediate values of both ℓ and γ are preferred. In the present system, there are few degrees of freedom, and the robust controllers do not provide much beyond what the optimal controllers provide. Notice, for example, the similar weights K and the similar transfer function norms attained with the $\ell=0.025$, $\gamma=\infty$ (''optimal'') case in Table I and the $\ell=10$, $\gamma=17.5$ (''robust'') case in Table II. This similarity in performance of the opti-

mal and robust controllers is in sharp contrast with the results of the high-dimensional, highly nonorthogonal problems studied in the transition control problem of Ref. 22, in which the noncooperative aspect of the controller formulation is much more significant.

Appendix B derives sufficient conditions on the feedback K for boundedness of the closed-loop nonlinear system which is obtained by application of the linear feedback Eq. (5a) to the undisturbed (i.e., $\mathbf{w}=\mathbf{0}$) nonlinear plant Eq. (2a). For control feedback determined from Eq. (5), which happens to satisfy these conditions, as shown in Fig. 5, direct application of linear feedback stabilizes both the desired state $\bar{\mathbf{x}}$ (indicated by the black trajectories of Fig. 5) and an undesired state $\bar{\mathbf{x}}'_c$ (indicated by the green trajectories of Fig. 5). This undesired stabilized state $\bar{\mathbf{x}}'_c$, given by

$$\bar{\mathbf{x}}'_c = \begin{pmatrix} -c_2 \\ -c_2 \\ -1 \end{pmatrix},$$

where $c_2=\sqrt{b(r-1)}-b(k_1+k_2)$, is near the aforementioned point $\bar{\mathbf{x}}'$ for small values of K. An unstable manifold exists between these two stabilized points, as indicated by the contorted blue/red surfaces in Fig. 5. Any initial state on the blue side of this manifold will converge to the desired state, and any initial state on the red side of this manifold will converge to the undesired state. It is mathematically possible that an unstable chaotic system trajectory still exists which is confined to the manifold separating these two regions of attraction. In a practical (disturbed) system, however, the state will never remain on this unstable manifold. Note that the unstable manifold includes the $x_1=x_2=0$ axis, which is indicated with white lines in Fig. 5.

As seen in Fig. 5, for increased feedback magnitude K (e.g., decreased ℓ), the undesired stabilized state $\bar{\mathbf{x}}'_c$ moves farther from the origin, and the domain of convergence of the undesired state remains large; the closed-loop system eventually becomes unbounded for sufficiently large feedback K. Some form of nonlinearity in the feedback rule is required to eliminate this undesired behavior. An effective technique is to apply control of the form

$$\mathbf{u}=H(R-|\mathbf{x}-\bar{\mathbf{x}}|)K\xi, \quad H(\zeta)=\begin{cases} 0 & \text{for } \zeta\leq0 \\ 1 & \text{for } \zeta>0, \end{cases}$$

such that the control is turned on only when the state $\mathbf{x}(t)$ is inside a sphere of radius R, centered at $\bar{\mathbf{x}}$, completely con-
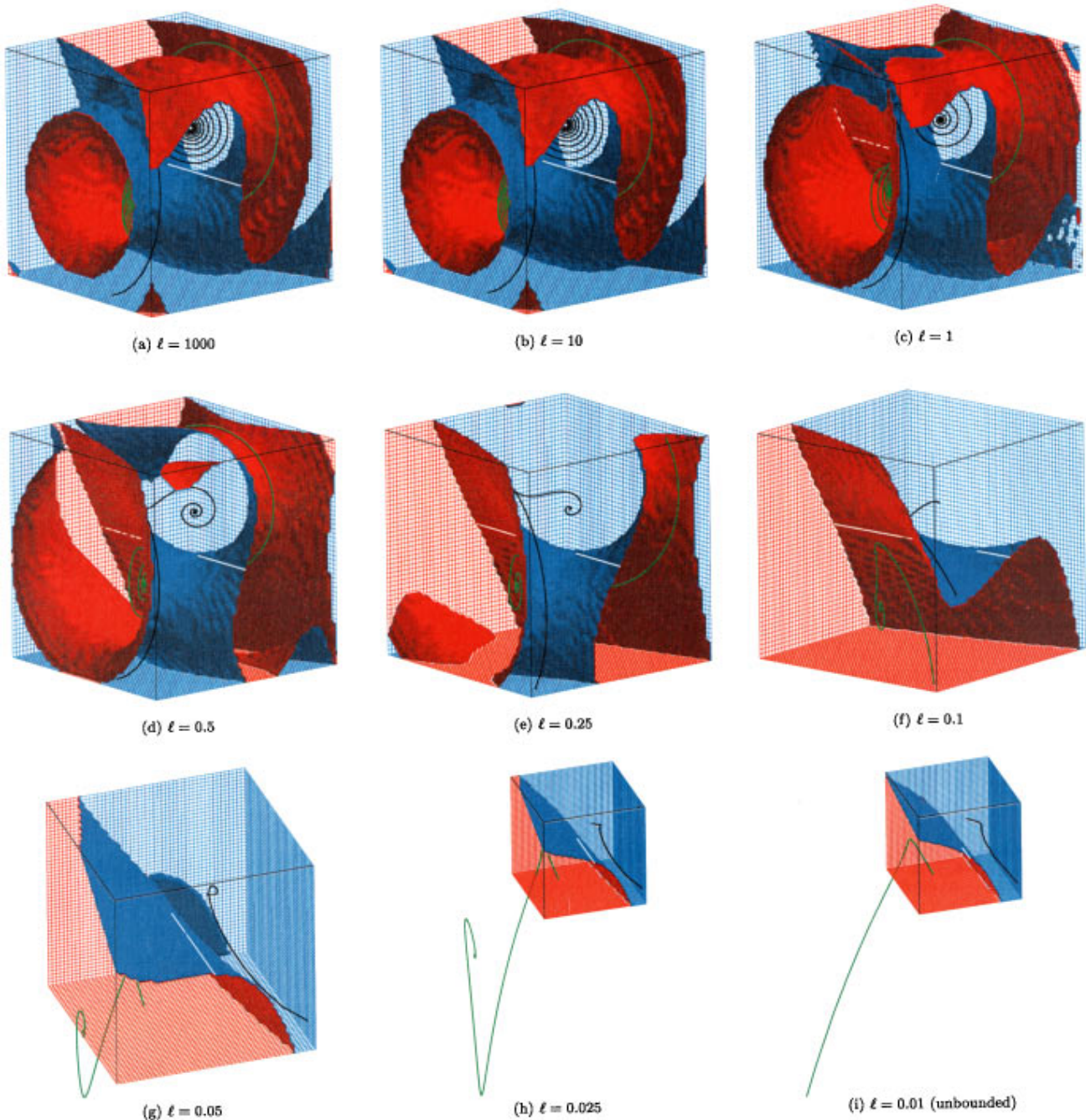
FIG. 5. Regions of attraction of desired (blue) and undesired (red) stationary points in linearly controlled convection system and typical trajectories in each region (black and green, respectively). The cubical domain illustrated is $\Omega=(-25,25)^3$ in all nine subfigures; for clarity, slightly different viewpoints are used in each subfigure.

tained in the domain of convergence of the desired stationary point in the linearly controlled system. Such a subdomain is denoted by a violet sphere in Fig. 6(a). The chaotic dynamics of the uncontrolled system will bring the system into this subdomain in finite time, as depicted by Fig. 6(b), after which control may be applied to ''catch'' the state at the desired equilibrium point. Similar switched approaches were recommended by Vincent ard Yu,[17] Wang and Abed,[19] and Vincent[15] for the Lorenz problem, and may also be applied to swing up and catch an inverted pendulum, as demonstrated by Malmborg, Bernhardsson, and Åström.[28] The key to the effectiveness of this approach is the determination of a

feedback control which makes the subdomain in which the linear control may be applied successfully as large as possible, so that the uncontrolled state $\mathbf{x}(t)$, moving along the attractor of the system, enters this subdomain in a short amount of time.[15]

IV. DETERMINATION OF AN EFFECTIVE STATE-ESTIMATION STRATEGY

When full state information is not available, one may first develop a state estimate based on the available state measurements, then feed this state estimate back through a

(a)   (b)
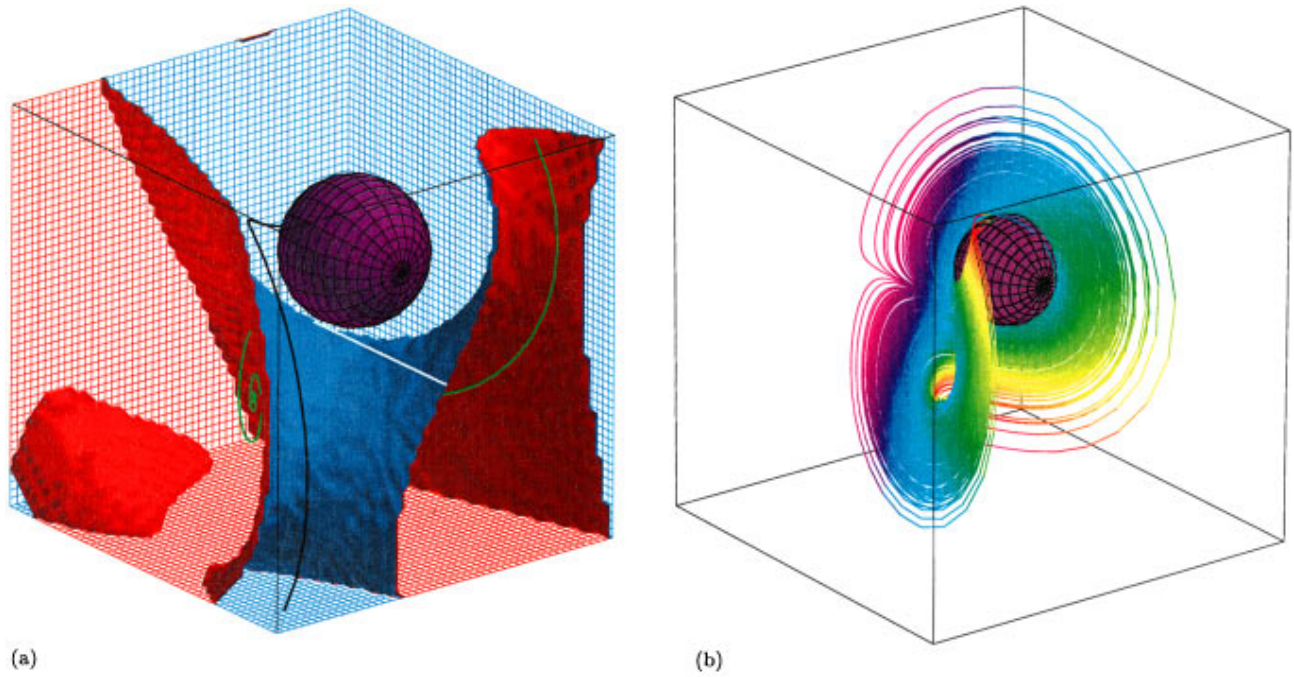
FIG. 6. Combination of the linear controller with an on/off switch. No control is applied when the state is outside the violet subdomain shown. The chaotic uncontrolled system eventually brings the state inside the subdomain shown. Linear control is then applied to ''catch'' the system, drawing it to the desired stabilized state. (a) Definition of a subdomain (violet) completely contained in the (blue) domain of convergence of the desired fixed point when linear optimal control with $\ell = 0.25$ is applied. It is possible to define a subdomain so contained which is larger than the example shown. (b) The subdomain defined (violet) contains a substantial portion of the chaotic attractor of the uncontrolled system. Thus the uncontrolled system will eventually move inside the subdomain where linear control is effective.

full-state controller, such as one of the controllers of Sec. III, to control the system. This chapter discusses how to determine an effective state estimator for the present problem. Details of how the synthesized estimator/controller is assembled are given in Sec. V.

A reasonable requirement of the state estimator is that its dynamics be at least similar to the dynamics of the state itself when no feedback is applied. To achieve this, the state estimator itself must be nonlinear. Since the state equation (2a) and the measurement equation (2b) are well known in the present problem, we will model them closely in our estimator equations such that

$$\dot{\hat{\mathbf{x}}} = A\hat{\mathbf{x}} + N(\hat{\mathbf{x}}) + B_2\mathbf{u} + \mathbf{r} - \hat{\mathbf{u}}, \tag{6a}$$

$$\hat{\mathbf{y}} = C_2\hat{\mathbf{x}}. \tag{6b}$$

The disturbance $\mathbf{w}$ that drives the flow system Eq. (2), which is unmeasurable, is not available to force the model system Eq. (6). Instead, a forcing term $\hat{\mathbf{u}}$ is computed based on the flow measurements $\mathbf{y}$ and added to the rhs of Eq. (6a) to force the state estimate $\hat{\mathbf{x}}$ in the estimator toward the state $\mathbf{x}$ itself, correcting for the state disturbances $B_1\mathbf{w}$ in Eq. (2a) while accounting for the measurement noise $D_{21}\mathbf{w}$ in Eq. (2b). The task at hand is to determine the feedback $\hat{\mathbf{u}}$ as a function of the measurements $\mathbf{y}$ such that this goal is attained. As in the previous section, the feedback will be determined by application of linear optimal/robust control theory, although this feedback is applied, in the end, to the *nonlinear* estimator given by Eq. (6). Since the state estimate is computed in the controlling electronics in any implemen-

tation, all three components of the model equation (6a) may be forced by the estimator feedback $\hat{\mathbf{u}} = (\hat{u}_1 \; \hat{u}_2 \; \hat{u}_3)^*$ with no difficulty in the implementation.

Consider the deviations $\boldsymbol{\eta}$ and $\hat{\boldsymbol{\eta}}$ of the state $\mathbf{x}$ and the state estimate $\hat{\mathbf{x}}$ from some (as yet undetermined) reference state $\tilde{\mathbf{x}}$ such that

$$\boldsymbol{\eta} \triangleq \mathbf{x} - \tilde{\mathbf{x}} \quad \text{and} \quad \hat{\boldsymbol{\eta}} \triangleq \hat{\mathbf{x}} - \tilde{\mathbf{x}}. \tag{7}$$

The equations governing $\boldsymbol{\eta}$ and $\hat{\boldsymbol{\eta}}$ are easily derived from Eqs. (2a) and (6a) such that

$$\dot{\boldsymbol{\eta}} = \tilde{A}\boldsymbol{\eta} + N(\boldsymbol{\eta}) + B_1\mathbf{w} + B_2\mathbf{u} + \tilde{\mathbf{r}}, \tag{8a}$$

$$\dot{\hat{\boldsymbol{\eta}}} = \tilde{A}\hat{\boldsymbol{\eta}} + N(\hat{\boldsymbol{\eta}}) \qquad\quad + B_2\mathbf{u} + \tilde{\mathbf{r}} - \hat{\mathbf{u}}, \tag{8b}$$

where the linearized system matrix $\tilde{A}$ and the constant vector $\tilde{\mathbf{r}}$ take the form

$$\tilde{A} \triangleq A + \begin{pmatrix} 0 & 0 & 0 \\ -\tilde{x}_3 & 0 & -\tilde{x}_1 \\ \tilde{x}_2 & \tilde{x}_1 & 0 \end{pmatrix}, \quad \tilde{\mathbf{r}} \triangleq A\tilde{\mathbf{x}} + N(\tilde{\mathbf{x}}) + \mathbf{r}.$$

Note that $\tilde{\mathbf{x}}$ need not be a stationary point, and thus $\tilde{\mathbf{r}}$ is not necessarily zero. Defining the estimation error $\mathbf{x}_e \triangleq \mathbf{x} - \hat{\mathbf{x}} = \boldsymbol{\eta} - \hat{\boldsymbol{\eta}}$ and the measurement error $\mathbf{y}_e \triangleq \mathbf{y} - \hat{\mathbf{y}}$ and subtracting Eq. (8b) from Eq. (8a) and Eq. (6b) from Eq. (2b), it is seen that $\mathbf{x}_e$ and $\mathbf{y}_e$ obey the equations

$$\dot{\mathbf{x}}_e = \tilde{A}\mathbf{x}_e + N(\boldsymbol{\eta}) - N(\hat{\boldsymbol{\eta}}) + B_1\mathbf{w} + \hat{\mathbf{u}}, \tag{9a}$$

$$\mathbf{y}_e = C_2\mathbf{x}_e + D_{21}\mathbf{w}. \tag{9b}$$

TABLE III. Optimal estimator (a.k.a. Kalman–Bucy filter) feedback gains ($\gamma=\infty$), Lyapunov exponent characterizing estimator convergence to uncontrolled state, and linear disturbance rejection near desired fixed point. The Lyapunov exponent κ_∞ denotes the exponential rate of convergence ($\kappa_\infty<0$) or divergence ($\kappa_\infty>0$) of the state estimate to the state as the state moves on the attractor when the estimation error $\mathbf{x}_e$ is small. Transfer function norms reported measure linearized response, near $\mathbf{x}=\hat{\mathbf{x}}=\overline{\mathbf{x}}$, of estimator error to state disturbances, though the estimator feedback was designed with linear theory by linearization about $\mathbf{x}=\hat{\mathbf{x}}=\mathbf{0}$ (i.e., transfer function norms are reported at conditions which are off the design point). Necessary conditions for effective estimator behavior are: (a) κ_∞ must be negative, and (b) the transfer function norms reported must be bounded.

α	L^*			κ_∞	$\|T_{\mathbf{x}_e\mathbf{w}}\|_2$	$\|T_{\mathbf{x}_e\mathbf{w}}\|_\infty$	$\|T_{\hat{\mathbf{u}}\mathbf{w}}\|_2$
10	$(-0.0040$	-0.0050	$0.0)$	0.70	∞	∞	∞
1	$(-0.3060$	-0.4142	$0.0)$	0.45	∞	∞	∞
0.50	$(-0.7929$	-1.2361	$0.0)$	0.04	1.690	2.599	1.555
0.25	$(-1.5379$	-3.1231	$0.0)$	-1.04	0.977	0.777	2.049
0.10	$(-2.5765$	-9.0499	$0.0)$	-3.95	0.747	0.401	3.384
0.050	$(-3.1675$	-19.0250	$0.0)$	-3.67	0.784	0.602	4.927
0.025	$(-3.5456$	-39.0125	$0.0)$	-1.82	0.913	0.915	6.851
0.010	$(-3.8077$	-99.0050	$0.0)$	0.01	1.101	1.361	9.814

The nonlinear term in this equation may be written

$$N(\boldsymbol{\eta})-N(\hat{\boldsymbol{\eta}})=M(\hat{\boldsymbol{\eta}})\mathbf{x}_e+N(\mathbf{x}_e),$$
$$=M(\boldsymbol{\eta})\mathbf{x}_e-N(\mathbf{x}_e), \tag{10}$$

where

$$M(\boldsymbol{\eta})=\begin{pmatrix} 0 & 0 & 0 \\ -\eta_3 & 0 & -\eta_1 \\ \eta_2 & \eta_1 & 0 \end{pmatrix}.$$

For sufficiently small $\boldsymbol{\eta}$ and $\mathbf{x}_e$, the linear terms of Eq. (9a) dominate the nonlinear term $N(\boldsymbol{\eta})-N(\hat{\boldsymbol{\eta}})$ [see Eq. (10)]. Thus for sufficiently small estimator error $\mathbf{x}_e$ *and* for the state $\mathbf{x}$ in a sufficiently small neighborhood of the reference state $\widetilde{\mathbf{x}}$, the estimator feedback $\hat{\mathbf{u}}$ minimizing the estimation error $\mathbf{x}_e$ may be determined by analysis of just the linear terms of Eq. (9).

Linear estimator feedback of the form

$$\hat{\mathbf{u}}=L\mathbf{y}_e=L(\mathbf{y}-\hat{\mathbf{y}}) \tag{11a}$$

solving the dual of the noncooperative game discussed in Sec. III for the linearization of the system Eq. (9) governing the estimation error $\mathbf{x}_e$ is given by the estimator feedback

$$L=-\frac{1}{\alpha^2}YC_2^*, \tag{11b}$$

where

$$Y=\text{Ric}\begin{pmatrix} \widetilde{A}^* & \dfrac{1}{\gamma^2}C_1^*C_1-\dfrac{1}{\alpha^2}C_2^*C_2 \\ -B_1B_1^* & -\widetilde{A} \end{pmatrix}, \tag{11c}$$

in accordance with standard linear theory.[24–26,22] Note that an ''optimal estimator,'' determined with $\gamma=\infty$, is usually referred to as a Kalman–Bucy filter. Resulting feedback matrices L for representative α and γ are given in Tables III and IV.

The linear (i.e., small) disturbance rejection of the closed-loop system Eq. (9) with the estimator feedback Eq. (11a) applied, given that the state $\mathbf{x}$ and the state estimate $\hat{\mathbf{x}}$ are near a known reference point, is (again) quantified by the appropriate transfer function norms.[27,22] In short,

$\|T_{\mathbf{x}_e\mathbf{w}}\|_2$ measures the rms value of the estimation error $\mathbf{x}_e$ in response to small white Gaussian disturbances $\mathbf{w}$,

$\|T_{\mathbf{x}_e\mathbf{w}}\|_\infty$ measures the rms value of the estimation error $\mathbf{x}_e$ in response to small disturbances $\mathbf{w}$ with the worst-case structure, and

$\|T_{\hat{\mathbf{u}}\mathbf{w}}\|_2$ measures the rms value of the estimator feedback $\hat{\mathbf{u}}$ in response to small white Gaussian disturbances $\mathbf{w}$.

The dependence of the performance of the estimation error system Eq. (9) on α and γ near the design point $\mathbf{x}\approx\hat{\mathbf{x}}\approx\widetilde{\mathbf{x}}$ is similar to the dependence of the design-point perfor-

TABLE IV. Robust estimator feedback gains ($\alpha=1$), Lyapunov exponent characterizing estimator convergence to uncontrolled state, and linear disturbance rejection near desired fixed point (see legend of Table III).

γ	L^*			κ_∞	$\|T_{\mathbf{x}_e\mathbf{w}}\|_2$	$\|T_{\mathbf{x}_e\mathbf{w}}\|_\infty$	$\|T_{\hat{\mathbf{u}}\mathbf{w}}\|_2$
∞	$(-0.3060$	-0.4142	$0.0)$	0.45	∞	∞	∞
2	$(-0.3384$	-0.4413	$0.0)$	0.44	∞	∞	∞
1.5	$(-0.3729$	-0.4696	$0.0)$	0.43	∞	∞	∞
1.1	$(-0.5091$	-0.5781	$0.0)$	0.38	4.778	21.57	2.326
1.02	$(-0.7062$	-0.7294	$0.0)$	0.29	2.597	6.290	1.670
$\gamma_0\approx1.016$	$(-0.7879$	-0.7909	$0.0)$	0.24	2.292	4.868	1.621

mance of the controlled system on ℓ and γ studied in Sec. III. The estimators summarized in Tables III and IV are designed with the feedback L determined according to Eq. (11) with $\tilde{\mathbf{x}}=0$. In Tables III and IV, we investigate the linear disturbance rejection of the closed-loop estimation error system near the desired fixed point $\mathbf{x} \approx \hat{\mathbf{x}} \approx \overline{\mathbf{x}}$, conditions which are *off* the design point for the estimator. For large α, the feedback determined is not sufficient to stabilize the estimator near the desired fixed point $\mathbf{x} \approx \hat{\mathbf{x}} \approx \overline{\mathbf{x}}$, and the transfer function norms reported are unbounded. Decreasing the parameter α results in increased estimator feedback gains L and eventually stabilizes the estimation error near the desired fixed point. This results in finite values of the transfer function norms reported in Table III for $\alpha \leq 0.5$. Decreasing the parameter α from 0.5 to 0.1 results in increased estimator feedback ($\|T_{\hat{\mathbf{u}}\mathbf{w}}\|_2$) to account for disturbances more rapidly, thereby resulting in a smaller response of the estimation error to Gaussian disturbances ($\|T_{\mathbf{x}_e\mathbf{w}}\|_2$). The worst-case response of the estimation error ($\|T_{\mathbf{x}_e\mathbf{w}}\|_\infty$) in this problem, which has few degrees of freedom, follows trends which closely match the estimation error response to Gaussian disturbances ($\|T_{\mathbf{x}_e\mathbf{w}}\|_2$), and introducing the robust component (Table IV) does not provide much beyond what the optimal approach can provide. The large feedback gains L for the estimators with $\alpha < 0.1$ are not effective in reducing further the system response under these off-design conditions; as for the controller, intermediate values of both α and γ are preferred.

By applying the linear measurement feedback Eq. (11a) to the undisturbed (i.e., $\mathbf{w}=0$) estimation error equations (9), noting Eq. (10), the closed-loop equation for the estimation error may be written in the form

$$\dot{\mathbf{x}}_e = (\tilde{A} + LC_2)\mathbf{x}_e - N(\mathbf{x}_e) + M(\boldsymbol{\eta}(t))\mathbf{x}_e ,$$
$$= (A + LC_2 + M(\mathbf{x}(t)))\mathbf{x}_e - N(\mathbf{x}_e). \qquad (12)$$

Conservative sufficient conditions for convergence of the nonlinear closed-loop system Eq. (12) are established in Appendix C. Unfortunately, it does not appear possible to select time-invariant linear estimator feedback L such that the estimator error decreases uniformly as the uncontrolled state $\mathbf{x}(t)$ moves along the trajectory of the attractor, as the term $M(\mathbf{x}(t))$ is destabilizing over a portion of the attractor. However, this does not imply that the estimator will necessarily diverge; effective estimators may still be found, as will now be shown.

The convergence or divergence of the state estimator for the uncontrolled system when the estimation error $\mathbf{x}_e$ is small may be made precise by extensions of the Lyapunov exponent λ_∞ and the local Lyapunov exponent $\lambda_\epsilon(\mathbf{x}(t))$ used to characterize the uncontrolled system in Sec. II A. Consider an infinitesimal perturbation $\delta\mathbf{x}_e(0)$ of the state estimator such that $|\delta\mathbf{x}_e(0)| = |\mathbf{x}(0) - \hat{\mathbf{x}}(0)| \ll 1$. The perturbation $\delta\mathbf{x}_e(t)$ evolves according to the linearization of Eq. (12), which is given by

$$\dot{\delta\mathbf{x}}_e = (A + LC_2 + M(\mathbf{x}(t)))\delta\mathbf{x}_e .$$

The Lyapunov exponent of the state estimation error, κ_∞, is defined as

$$\kappa_\infty = \lim_{T \to \infty} \frac{1}{T} \log \frac{\|\delta\mathbf{x}_e(T)\|}{\|\delta\mathbf{x}_e(0)\|}$$

for almost all initial states $\mathbf{x}(0)$ and initial infinitesimal estimator perturbations $\delta\mathbf{x}_e(0)$, in a manner analogous to the Lyapunov exponent λ_∞ of the uncontrolled system. The Lyapunov exponent of the state estimation error, κ_∞, thus measures the exponential rate of convergence ($\kappa_\infty < 0$) or divergence ($\kappa_\infty > 0$) of the state estimator when averaged over long time intervals ($T \to \infty$). Calculated values of the Lyapunov exponent κ_∞ for the present estimators are tabulated in Tables III and IV. The local Lyapunov exponent of the state estimation error, $\kappa_\epsilon(\mathbf{x}(t))$, is defined as

$$\kappa_\epsilon(\mathbf{x}(t)) = \lim_{T \to 0} \frac{1}{T} \log \frac{\|\delta\mathbf{x}_e(t+T)\|}{\|\delta\mathbf{x}_e(t)\|}$$

for almost all initial states $\mathbf{x}(0)$ and initial infinitesimal estimator perturbations $\delta\mathbf{x}_e(0)$ and for t sufficiently large, in a manner analogous to the local Lyapunov exponent $\lambda_\epsilon(\mathbf{x}(t))$ of the uncontrolled system. The local Lyapunov exponent of the state estimation error, $\kappa_\epsilon(\mathbf{x}(t))$, thus measures the local exponential rate of convergence or divergence of state and the state estimate when the estimation error is small. The Lyapunov exponent κ_∞ is the long-time average along the system trajectory $\mathbf{x}(t)$ of the local Lyapunov exponent $\kappa_\epsilon(\mathbf{x}(t))$ (see Fig. 7). As the estimator equation (6a) accurately models the state equation (2a), the Lyapunov exponent for the estimator κ_∞ reduces to the Lyapunov exponent for the uncontrolled state $\lambda_\infty = 0.707$ when the estimator feedback L is made small, as shown in Table III.

It is demonstrated in simulations (see, for example, Fig. 8) that, for α sufficiently small that $\kappa_\infty < 0$ (Table III), the estimator feedback stabilizes the estimator error $\mathbf{x}_e$ to zero even for initial conditions of the estimation error $\mathbf{x}_e(0)$ which are not small. As opposed to the control problem, no undesired stabilized states other than $\mathbf{x}_e = 0$ were detected in the closed-loop nonlinear system for the estimation error.

It was found [compare Fig. 7(b) and 7(c)] that choosing a (time-invariant) reference state $\tilde{\mathbf{x}}$ at the origin, which is the approximate "center of mass" of the orbits of the uncontrolled system [Fig. 2(a)–(c)], gave the best estimator performance for the range of initial conditions tested. This is reasonable, as the reference state $\tilde{\mathbf{x}}$, about which we linearize the system to determine the estimator feedback, should be as close as possible to the state $\mathbf{x}(t)$ at any instant for the linearization of the estimator error equation [specifically, the neglect of $M(\boldsymbol{\eta})$ in Eq. (12)] to be valid.

It was also found [compare Fig. 7(b) and 7(c)] that the nonlinear term $N(\hat{\mathbf{x}})$ in the estimator Eq. (6a) is essential for good estimator performance. Without it, the equation for a small perturbation $\delta\mathbf{x}_e(t)$ of the estimator (when we take $\tilde{\mathbf{x}} = 0$) takes the form

$$\dot{\delta\mathbf{x}}_e = (A + LC_2)\delta\mathbf{x}_e + N(\mathbf{x}(t)),$$

where the nonlinear term $N(\mathbf{x}(t))$ is not small as the state $\mathbf{x}(t)$ moves on the attractor. The linear estimator feedback $LC_2\delta\mathbf{x}_e$, which is proportional to the size of the estimation error perturbation, is not sufficient to stabilize this term. The
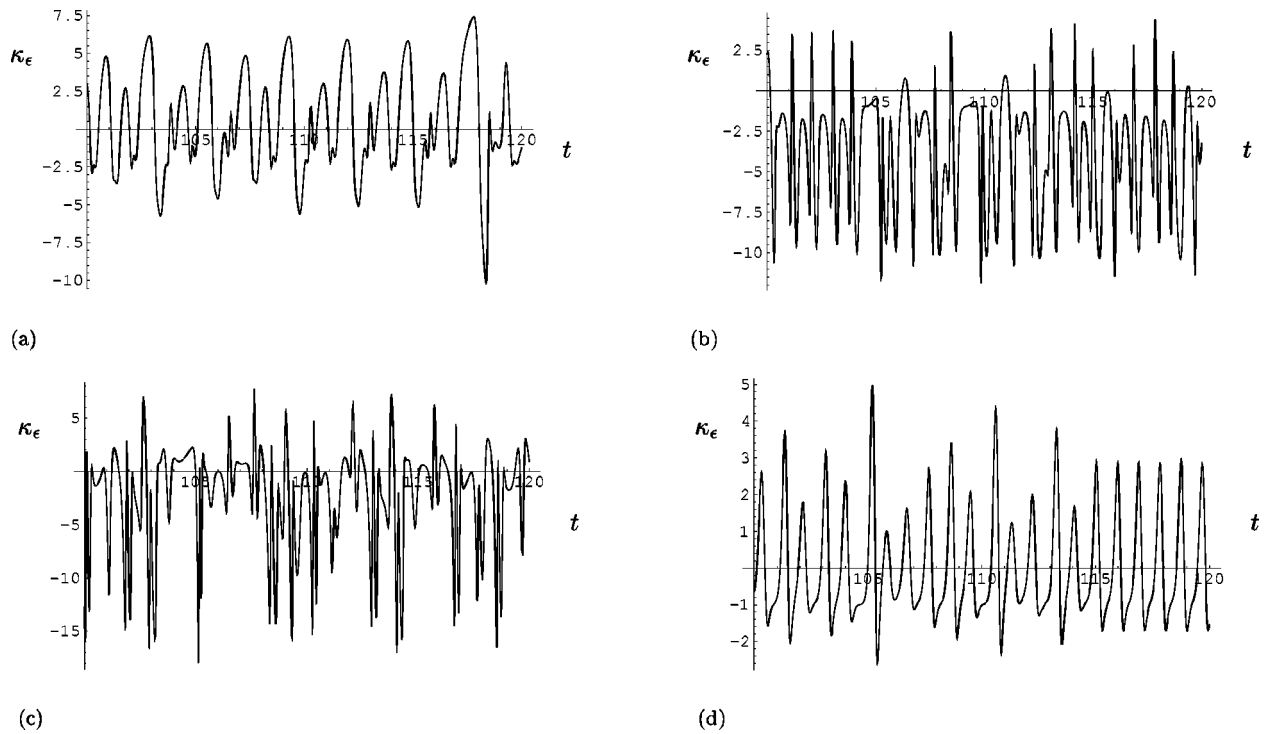
(a)

(b)

(c)

(d)

FIG. 7. Local Lyapunov exponent $\kappa_\epsilon(t)$ describing the local growth or attenuation of small perturbations of the estimation error $\mathbf{x}_e(t)$ in the closed-loop system for the state estimator as the state $\mathbf{x}(t)$ moves along the attractor. (a) Estimator designed with $\alpha = 1.0$, $\tilde{\mathbf{x}} = \mathbf{0}$. The value of the Lyapunov exponent κ_∞, which is the average value of the local Lyapunov exponent κ_ϵ plotted, is $\kappa_\infty = 0.45 > 0$. This indicates that the state estimator is unstable ($\kappa_\epsilon > 0$) more than it is stable ($\kappa_\epsilon < 0$), and thus the state estimate will not converge to the uncontrolled state. (b) Estimator designed with $\alpha = 0.1$, $\tilde{\mathbf{x}} = \mathbf{0}$. The value of the Lyapunov exponent is $\kappa_\infty = -3.95 < 0$. This indicates that the state estimator is stable more than it is unstable, and thus the state estimate will converge to the uncontrolled state when $\mathbf{x}_e$ is small. Note that estimator convergence is attained even though the estimator error does not decrease uniformly over the entire path of the attractor. (c) Estimator designed with $\alpha = 0.1$, $\tilde{\mathbf{x}} = \bar{\mathbf{x}}$. Lyapunov exponent $\kappa_\infty = -2.33 < 0$. It is found that linear estimator feedback designed with $\tilde{\mathbf{x}} = \mathbf{0}$ has better convergence properties [cf. (b)]. (d) Estimator designed with $\alpha = 0.1$, $\tilde{\mathbf{x}} = \mathbf{0}$, and the nonlinear term dropped from the estimator equation (6). Lyapunov exponent $\kappa_\infty = 0.01$. The nonlinear term in the estimator is essential for good performance [cf. (b)].

estimator will continually be disrupted if the nonlinear term $N(\hat{\mathbf{x}})$ is not included in the equation for the estimator Eq. (6).

Better performance may be obtained in flow systems which prove to be more difficult to estimate using a *gain scheduling* approach to select the most suitable estimator feedback gains. Note that the simple switching function $H(\zeta)$ used for the controller feedback in the previous section is a crude example of a simple gain scheduling approach. For the estimator, a gain scheduling approach might entail a reference state which is a function of time, with the linear feed-
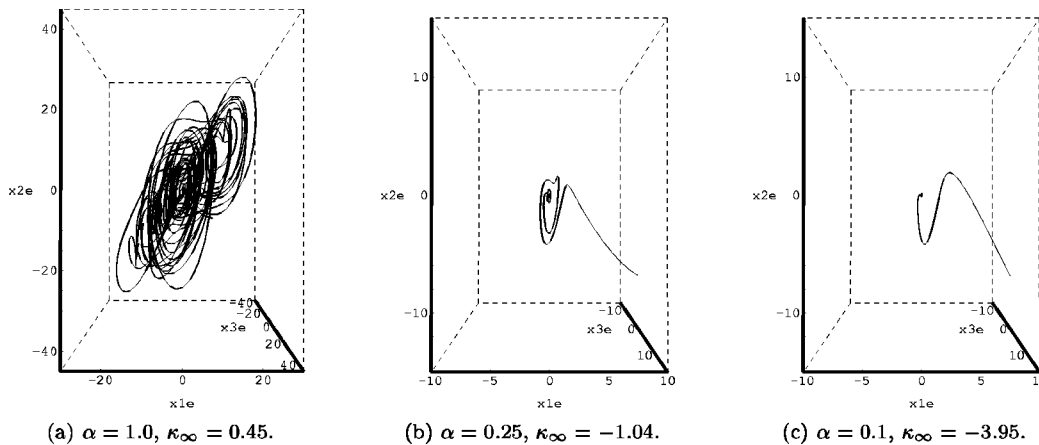

(a) $\alpha = 1.0$, $\kappa_\infty = 0.45$.   (b) $\alpha = 0.25$, $\kappa_\infty = -1.04$.   (c) $\alpha = 0.1$, $\kappa_\infty = -3.95$.

FIG. 8. Trajectory of the estimation error $\mathbf{x}_e(t)$ for estimators determined with $\tilde{\mathbf{x}} = \mathbf{0}$ and three different values of α when applied to the uncontrolled, undisturbed convection system. The initial conditions on the state, $\mathbf{x}(0) = (5\ 1\ 0)^*$, and the state estimate, $\hat{\mathbf{x}}(0) = (-5\ 10\ 0)^*$, are separated significantly in these simulations. Even so, for estimators with $\kappa_\infty < 0$, the estimator feedback $\hat{\mathbf{u}}$ rapidly brings the state estimate $\hat{\mathbf{x}}$ in close proximity to the state $\mathbf{x}$ based on measurements of x_2 only. Such behavior is seen with all initial conditions tested. The approach of the estimated state to the actual state is more rapid for estimators with more negative values of κ_∞. After the state and the estimate are brought into proximity, nonlinear estimators with $\kappa_\infty < 0$ accurately track the chaotic trajectory of the state with little further estimator feedback required.

back gains $L(t)$ recomputed as the system evolves using the linearization $\tilde{\mathbf{x}}(t) = \hat{\mathbf{x}}(t)$ in the spirit of a linear parameter-varying (LPV) procedure. With such an approach, $\hat{\boldsymbol{\eta}}(t)$ and $M(\hat{\boldsymbol{\eta}}(t))$ are identically zero, and stability of the estimator error to small disturbances anywhere on the attractor is easily established by the local linear stability of the closed-loop system matrix $\tilde{A}(t) + L(t)C_2$. A gain scheduling approach, however, is more difficult to implement than constant-gain feedback, requiring on-line computation of the estimator Riccati equation (11c), and is *not* required to stabilize the estimator error in the present system, given that the constant estimator feedback L selected is sufficient to provide $\kappa_\infty < 0$, as discussed above.

V. PRACTICAL CONTROL APPROACH

It is straightforward to combine the estimators and controllers of the two previous sections to obtain an estimator-based controller which may be implemented based on limited noisy measurements. The flow of information in this approach is illustrated schematically by the following standard block diagram.
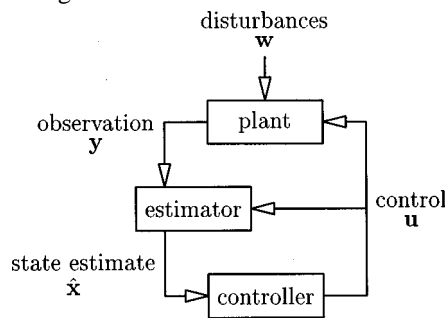
The plant, forced by external disturbances, has an internal state $\mathbf{x}$ which cannot be observed. Instead, a noisy observation $\mathbf{y}$ is made and an estimate of the state $\hat{\mathbf{x}}$ determined. This state estimate is then fed through the controller to determine the control $\mathbf{u}$ to be applied on the plant to regulate $\mathbf{x}$ to zero.

To summarize, the equations governing the plant (replaced in the implementation by the apparatus itself) are

$$\dot{\mathbf{x}} = A\mathbf{x} + N(\mathbf{x}) + B_1\mathbf{w} + B_2\mathbf{u} + \mathbf{r},$$

$$\mathbf{y} = C_2\mathbf{x} + D_{21}\mathbf{w},$$

the (nonlinear) equations for the estimator (updated by the measurements $\mathbf{y}$ only) are

$$\dot{\hat{\mathbf{x}}} = A\hat{\mathbf{x}} + N(\hat{\mathbf{x}}) + B_2\mathbf{u} + \mathbf{r} - \hat{\mathbf{u}},$$

$$\hat{\mathbf{y}} = C_2\hat{\mathbf{x}},$$

$$\hat{\mathbf{u}} = H(t - t_1)L(\mathbf{y} - \hat{\mathbf{y}}),$$

and the equation for the controller (based now on the state estimate $\hat{\mathbf{x}}$) is

$$\mathbf{u} = H(t - t_2)H(R - |\hat{\mathbf{x}} - \bar{\mathbf{x}}|)K(\hat{\mathbf{x}} - \bar{\mathbf{x}}).$$

Values of K and L have been computed by application of linear control theory to the appropriate linearized problems and are reported in Tables I–IV. Three parameters $\{\gamma, \alpha, \ell\}$ may be used to scale the magnitude of the estimator and controller feedback appropriately for particular implementa-

tions. Note that estimator feedback is turned on only after an amount of time t_1 has elapsed which is sufficiently large that the state $\mathbf{x}(t)$ is near the attractor, after which the convergence of the estimator has been thoroughly verified, and control feedback is turned on only after both

(i)   an amount of time $t_2 > t_1$ has elapsed which is sufficiently large that the state estimation error $\mathbf{x}_e(t) = \mathbf{x}(t) - \hat{\mathbf{x}}(t)$ is small, and

(ii) the state estimate $\hat{\mathbf{x}}(t)$ (and therefore the state $\mathbf{x}(t)$ itself) has meandered to a point within the subdomain, illustrated in Fig. 6, inside of which convergence of the linearly controlled system to the desired state is assured.

For this approach to be effective, the estimator must be able to both

(a)   track the uncontrolled state $\mathbf{x}(t)$ as it moves on the attractor, and

(b)   track small perturbations of the controlled state in the vicinity of the desired fixed point.

It is found by simulation that, when the appropriate controllers and estimators are selected, the approach described above converges from all initial conditions tested. A particular case tested in detail took $t_1 = 0$, $t_2 = 5$, $R = 9$, $\hat{\mathbf{x}}(0) = \mathbf{0}$, estimator feedback computed with $\alpha = 0.1$ and $\gamma = \infty$, controller feedback computed with $\ell = 0.25$ and $\gamma = \infty$, and sampled a large range of initial conditions $\mathbf{x}(0)$ within the absorbing ball of Fig. 2(d). The estimator converged properly and the control application successfully caught the state at the desired state in all cases tested.

VI. CONCLUSIONS AND RELATED QUESTIONS IN THE TURBULENCE PROBLEM

It has been demonstrated that, using linear optimal/robust control theory, the Lorenz equation may be estimated effectively based on partial state measurements and controlled effectively with limited control authority. Linear state feedback is found to be fully effective only when it is switched off while the state is far from the desired equilibrium point, relying on the attractor of the system to bring the state into a neighborhood of the equilibrium point before control is applied. Linear estimator feedback is found to be fully effective only when (a) the Lyapunov exponent of the state estimation error is negative, indicating that the state estimate converges to the uncontrolled state, and (b) the estimator is stable in the vicinity of the desired equilibrium point. Fundamental limitations in the control and estimation of a nonlinear system by linear feedback have been characterized.

For the present nonlinear problem, nonlinear feedback controllers may be constructed which are superior in terms of their global convergence to the linear controllers examined here. Wang and Abed[19] achieve effective control of the present system with a washout filter and control with a cubic nonlinearity, supplanting the linear controller Eq. (5) with

$$\dot{x}_4 = x_3 - k_1 x_4,$$

$$u = -k_2(x_3 - k_1 x_4)^3.$$

A controller of a similar form was implemented experimentally by Yuen and Bau.[21] Ezal, Pan, and Kokotovic[29] have shown that the integrator backstepping approach (which involves the recursive construction of appropriate Lyapunov functions for each scalar component of the governing equation) may be applied to compute nonlinear feedback controls for a certain class of nonlinear systems for global stabilization while maintaining local optimality. Systems that lend themselves to this approach may be written in the strict-feedback form

$$\dot{x}_1 = x_2 + f_1(x_1) + h_1(x_1)w,$$
$$\dot{x}_2 = x_3 + f_2(x_1, x_2) + h_1(x_1, x_2)w,$$
$$\vdots$$
$$\dot{x}_n = u + f_n(x_1, \cdots, x_n) + h_n(x_1, \cdots, x_n)w.$$

Such methods of constructive Lyapunov stabilization[30] do extend to the Lorenz equation, at least in problems in which the control is applied to the equation for x_2 (the left/right temperature difference), as considered by Jankovic.[31] In the problem considered in the present paper, control is applied to the equation for x_3 (the top/bottom temperature difference). This appears to be a slightly more difficult control problem: for instance, globally stabilizing linear controls, such as those found by Wan and Bernstein,[20] appear to be unavailable in the present case (see Appendix B). It remains to be seen whether or not the intriguing nonlinear approaches discussed above may be extended to more complex systems, such as those governed by the Navier–Stokes equation.

In this paper, we have focused our attention on the fundamental limitations inherent to the application of linear feedback control to the present nonlinear system, as we are considering the Lorenz system as a model for more complex systems for which appropriate nonlinear feedback approaches are not yet available. As quoted by Petar Kokotovic,[32] Richard Bellman is said to have compared one who designs linear controls for nonlinear systems with one who, ''having lost his watch in a dark alley, is searching for it under a lamp post.'' To pursue this metaphor further, we are, indeed, waiting at the lamp post with our present approach; however, due to the chaotic behavior of the Lorenz system, we are confident that our watch will roll into view in finite time. Important open questions remain:

(1) Are switched approaches, similar to the one required for the present convection problem, necessary for effective application of linear feedback to turbulence?
(2) If the answer to question (1) is positive, under what conditions does turbulence flow into the view of linear controls, and what linear control algorithms illuminate the largest area?
(3) If the conditions for the successful application of linear feedback to turbulence are overly restrictive, what forms of nonlinear feedback are best suited for the problem of turbulence?

To make these questions concrete, subcritical (i.e., low Reynolds number) turbulent channel flow is an appropriate testbed.[33] This flow is observed in simulation and experiment to have recurrent features, referred to as coherent structures,[34,35] characteristic of higher Reynolds number flows of practical engineering interest. The near-wall coherent structures are a major source of the turbulent cascade of energy, and may be eliminated by control actuation applied at the wall (blowing/suction). Globally stabilizing controls, however, are exceedingly difficult to determine and, to date, have been found only with nonlinear optimal control theory in an (entirely impractical) predictive control setting.[36] More practical control algorithms are necessary. At least three control approaches for this nonlinear problem come to mind:

(1) Design a linear optimal/robust controller for increased linear stability of the laminar flow,[22] possibly coupling with a reduced-order state estimator[37] updated with linear measurement feedback. Such an approach is a direct extension of the approach used in the present manuscript, and similar problems should be expected. Note that uncontrolled subcritical turbulent channel flow remains at all times far from the stable equilibrium point of laminar channel flow at the same bulk velocity. Thus the state of the uncontrolled system might never enter a subdomain inside of which the effectiveness of the linear controller can be assured [cf. Fig. 6(b)].

(2) Numerically optimize the undetermined coefficients in a simple (linear or nonlinear) output feedback rule for particular turbulent flow realizations, either with nonlinear optimal/robust control theory[38,39] or with a heuristic training algorithm such as a neural network.[40] Such optimizations must be performed on large ensembles of turbulent flows to achieve optimized *ad hoc* control rules which generalize to other turbulent flow realizations, and thus are numerically challenging to perform. Effective performance of such approaches can not be guaranteed, but can at least partially reduce the magnitude of the turbulent fluctuations.[40]

(3) Apply nonlinear feedback control theory for PDEs based on rigorous notions such as L2-gain and passivity[41,42] as such theory becomes available.

It is not certain which approach will most effectively bring turbulence into the light, and all three approaches will continue to be explored.

ACKNOWLEDGMENTS

APPENDIX A: BOUNDEDNESS OF THE STATE OF THE UNCONTROLLED SYSTEM

After an initial transient, the trajectory of the state **x** in the uncontrolled Lorenz system Eq. (1) ultimately becomes confined[1] to a bounded subspace of the three-dimensional

phase space $\{x_1, x_2, x_3\}$, as indicated in Fig. 2, approaching the set referred to as the attractor of the system. The boundedness of this attractor is now established.

Lemma 1. *Given the uncontrolled open-loop system for the state* $\mathbf{x}$, *of the form*

$$\dot{\mathbf{x}} = \begin{pmatrix} \sigma(x_2 - x_1) \\ -x_2 - x_1 x_3 \\ -b x_3 + x_1 x_2 - b\bar{u} \end{pmatrix} = A\mathbf{x} + N(\mathbf{x}) + \mathbf{r},$$

with

$$A \triangleq \begin{pmatrix} -\sigma & \sigma & 0 \\ 0 & -1 & 0 \\ 0 & 0 & -b \end{pmatrix}, \quad N(\mathbf{x}) \triangleq \begin{pmatrix} 0 \\ -x_1 x_3 \\ x_1 x_2 \end{pmatrix},$$

$$\mathbf{r} \triangleq \begin{pmatrix} 0 \\ 0 \\ -b\bar{u} \end{pmatrix},$$

for $\sigma \geq 1$, $0 < b < 2$, *and* $\bar{u} > 1$. *The existence of an absorbing ball may be established such that any trajectory of* $\mathbf{x}$ *originating outside of this ball will enter it in finite time, and any trajectory of* $\mathbf{x}$ *inside this ball will never leave it.*

Proof of Lemma 1. (Outlined by Sparrow.[9]) Define a Lyapunov function[41,43] V such that

$$V \triangleq \frac{1}{2}[\bar{u}x_1^2 + \sigma x_2^2 + \sigma(x_3 - \bar{u})^2].$$

Differentiating V, it is easily shown that

$$\dot{V} = \bar{u}x_1\dot{x}_1 + \sigma x_2\dot{x}_2 + \sigma(x_3 - \bar{u})\dot{x}_3$$

$$= -\sigma(\bar{u}x_1^2 + x_2^2 + b x_3^2 - b\bar{u}^2).$$

Note that $\dot{V} < 0$ everywhere outside an ellipsoidal domain D, where D is defined by

$$\frac{x_1^2}{b\bar{u}} + \frac{x_2^2}{b\bar{u}^2} + \frac{x_3^2}{\bar{u}^2} \leq 1 \quad \forall \mathbf{x} \in D.$$

Define an ellipsoidal domain E such that

$$\frac{x_1^2}{4\sigma\bar{u}} + \frac{x_2^2}{4\bar{u}^2} + \frac{(x_3 - \bar{u})^2}{4\bar{u}^2} \leq 1 + \epsilon \quad \forall \mathbf{x} \in E$$

for some small but finite $\epsilon > 0$. Note that V is constant on the surface of E, with larger values outside and smaller values inside. Since D [the smaller ellipsoid of Fig. 2(d)] is completely contained in E [the larger ellipsoid of Fig. 2(d)], it follows that $\dot{V} \leq -\delta(\epsilon)$ everywhere on the surface and outside of E, for some finite $\delta(\epsilon) > 0$. It follows directly from these two conditions that

(a) any trajectory of the system originating outside of E will enter it in finite time, and

(b) all trajectories pass *inward* through the boundary of E, so any trajectory of the system inside E will never leave it.

The surface of E is thus referred to as an "absorbing ball" of the state $\mathbf{x}$. □

APPENDIX B: BOUNDEDNESS OF THE STATE OF THE CONTROLLED SYSTEM

Lemma 2. *Given the linearly controlled closed-loop system for* $\boldsymbol{\eta} = \mathbf{x} - \tilde{\mathbf{x}}$, *the deviation of the state* $\mathbf{x}$ *from some (arbitrary) reference state* $\tilde{\mathbf{x}}$, *which may be written in the form*

$$\dot{\boldsymbol{\eta}} = (\tilde{A} + B_2 K)\boldsymbol{\eta} + N(\boldsymbol{\eta}) + \tilde{\mathbf{r}},$$

with

$$\tilde{A} + B_2 K \triangleq \begin{pmatrix} -\sigma & \sigma & 0 \\ -\tilde{x}_3 & -1 & -\tilde{x}_1 \\ -\tilde{x}_2 - b k_1 & \tilde{x}_1 - b k_2 & -b - b k_3 \end{pmatrix},$$

$$K^* \triangleq \begin{pmatrix} k_1 \\ k_2 \\ k_3 \end{pmatrix}, \quad \bar{\mathbf{x}} \triangleq \begin{pmatrix} \sqrt{b(\bar{u} - 1)} \\ \sqrt{b(\bar{u} - 1)} \\ -1 \end{pmatrix},$$

$$\tilde{\mathbf{r}} \triangleq A\tilde{\mathbf{x}} + N(\tilde{\mathbf{x}}) + \mathbf{r} + B_2 K(\tilde{\mathbf{x}} - \bar{\mathbf{x}}),$$

where A, $N(\cdot)$, $\mathbf{r}$, σ, b, *and* $\bar{u}$ *are defined as in Lemma 1. If* $k_3 > -(1+b)/b$ *and* $k_2^2 < 4(1+k_3)/b$, *the existence of an absorbing ball may be established such that any trajectory of* $\boldsymbol{\eta}$ *originating outside of this ball will enter it in finite time, and any trajectory of* $\boldsymbol{\eta}$ *inside this ball will never leave it.*

Proof of Lemma 2. Define a Lyapunov function V_c such that

$$V_c \triangleq \frac{1}{2}\boldsymbol{\eta}^*\boldsymbol{\eta}.$$

Differentiating V_c and noting that $\boldsymbol{\eta}^* N(\boldsymbol{\eta}) = 0$, it is easily shown that

$$\dot{V}_c = \boldsymbol{\eta}^*\dot{\boldsymbol{\eta}} = \boldsymbol{\eta}^*(\tilde{A} + B_2 K)\boldsymbol{\eta} + \boldsymbol{\eta}^*\tilde{\mathbf{r}}.$$

The nonzero part of the first term comes from the symmetric part of $\tilde{A} + B_2 K$, which is given by

$$S_c(\tilde{\mathbf{x}}) = \begin{pmatrix} -\sigma & \dfrac{\sigma - \tilde{x}_3}{2} & \dfrac{\tilde{x}_2 - b k_1}{2} \\ \dfrac{\sigma - \tilde{x}_3}{2} & -1 & \dfrac{-b k_2}{2} \\ \dfrac{\tilde{x}_2 - b k_1}{2} & \dfrac{-b k_2}{2} & -b - b k_3 \end{pmatrix}.$$

Define $\tilde{\mathbf{x}} \triangleq (0 \; b k_1 \; \sigma)^*$. With this value of $\tilde{\mathbf{x}}$, a sufficient condition for $S_c(\tilde{\mathbf{x}})$ to be negative definite is that the submatrix

$$\begin{pmatrix} -1 & \dfrac{-b k_2}{2} \\ \dfrac{-b k_2}{2} & -b - b k_3 \end{pmatrix}$$

has negative eigenvalues, which is true if

$$k_3 > -\frac{1+b}{b} \quad \text{and} \quad k_2^2 < \frac{4(1+k_3)}{b}. \tag{B1}$$

Note that these inequalities are satisfied by some, but not all, of the the values K computed by linear optimal/robust control theory and reported in Tables I and II.

Let λ_1 be the maximum eigenvalue of $S_c(\tilde{\mathbf{x}})$, and assume that the conditions of Eq. (B1) are satisfied (i.e., $\lambda_1 < 0$). It follows that

$$\dot{V}_c = \boldsymbol{\eta}^*(\tilde{A} + B_2 K)\boldsymbol{\eta} + \boldsymbol{\eta}^*\tilde{\mathbf{r}}$$
$$\leq \lambda_1 |\boldsymbol{\eta}|^2 + |\boldsymbol{\eta}||\tilde{\mathbf{r}}|.$$

Define a spherical domain E_c such that

$$|\boldsymbol{\eta}| \leq \left|\frac{\tilde{\mathbf{r}}}{\lambda_1}\right| + \epsilon \quad \forall \, \boldsymbol{\eta} \in E_c$$

for some small but finite $\epsilon > 0$. It follows that $\dot{V}_c \leq -\delta(\epsilon)$ everywhere on the surface and outside of E_c, for some finite $\delta(\epsilon) > 0$. Note that V_c is constant on the surface of the spherical domain E_c, with larger values outside and smaller values inside. It therefore follows, as in the proof of Lemma 1, that the surface of E_c is an absorbing ball of the controlled state $\boldsymbol{\eta} = \mathbf{x} - \tilde{\mathbf{x}}$.   □

If we take $\tilde{\mathbf{x}} = \bar{\mathbf{x}}$ in Lemma 2, it follows that $\tilde{\mathbf{r}} = \bar{\mathbf{r}} = \mathbf{0}$ (as in Sec. III). Thus if we could choose a K such that $S_c(\bar{\mathbf{x}})$ (i.e., the symmetric part of $\bar{A} + B_2 K$) had all negative eigenvalues, we could shrink the absorbing ball E_c to a small neighborhood ϵ of $\mathbf{x} = \bar{\mathbf{x}}$, and the desired fixed point would be globally asymptotically stable. Unfortunately, this is impossible, due to the fact that the submatrix

$$\begin{pmatrix} -\sigma & \dfrac{\sigma - \bar{x}_3}{2} \\ \dfrac{\sigma - \bar{x}_3}{2} & -1 \end{pmatrix}$$

has a positive eigenvalue in the present case. Note that, as other Lyapunov functions V_c may also be considered, this observation does not suffice to prove that no constant linear feedback matrix K exists which provides global asymptotic stability to $\bar{\mathbf{x}}$ in the present problem, though no such feedback has yet been found.

APPENDIX C: CONVERGENCE OF THE STATE ESTIMATION ERROR

Lemma 3. *Given the closed-loop system (with linear measurement feedback) for the state estimation error $\mathbf{x}_e = \mathbf{x} - \hat{\mathbf{x}}$, the deviation of the state $\mathbf{x}$ from the state estimate $\hat{\mathbf{x}}$, which may be written in the form*

$$\dot{\mathbf{x}}_e = (A + LC_2 + M(\mathbf{x}))\mathbf{x}_e - N(\mathbf{x}_e),$$

with

$$A + LC_2 \triangleq \begin{pmatrix} -\sigma & \sigma + l_1 & 0 \\ 0 & -1 + l_2 & 0 \\ 0 & l_3 & -b \end{pmatrix},$$

$$L \triangleq \begin{pmatrix} l_1 \\ l_2 \\ l_3 \end{pmatrix}, \quad M(\mathbf{x}) \triangleq \begin{pmatrix} 0 & 0 & 0 \\ -x_3 & 0 & -x_1 \\ x_2 & x_1 & 0 \end{pmatrix},$$

where A, $N(\cdot)$, σ, and b are defined as in Lemma 1. The L_2-norm of the state estimation error $\mathbf{x}_e$ decreases uniformly in time whenever the linear feedback L and the state $\mathbf{x}$ are

such that the eigenvalues of the symmetric part of $A + LC_2 + M(\mathbf{x})$ are negative.

Proof of Lemma 3. Define a Lyapunov function V_e such that

$$V_e \triangleq \frac{1}{2}\,\mathbf{x}_e^*\mathbf{x}_e.$$

Differentiating V_e and noting that $\mathbf{x}_e^* N(\mathbf{x}_e) = 0$, it is easily shown that

$$\dot{V}_e = \mathbf{x}_e^*\dot{\mathbf{x}}_e = \mathbf{x}_e^*(A + LC_2 + M(\mathbf{x}))\mathbf{x}_e.$$

The nonzero part of this expression comes from the symmetric part of $A + LC_2 + M(\mathbf{x})$, which is given by

$$S_e(\mathbf{x}) = \begin{pmatrix} -\sigma & \dfrac{\sigma + l_1 - x_3}{2} & \dfrac{x_2}{2} \\ \dfrac{\sigma + l_1 - x_3}{2} & -1 + l_2 & \dfrac{l_3}{2} \\ \dfrac{x_2}{2} & \dfrac{l_3}{2} & -b \end{pmatrix}.$$

Let E_e contain only those points in $\mathbf{x}$ for which, for a given L and for all $\mathbf{x} \in E_e$, all eigenvalues of $S_e(\mathbf{x})$ are negative. [A necessary and sufficient condition for all eigenvalues to be negative may be established by applying the Routh–Hurwitz criterion to the expression for $\det(\lambda I - S_e(\mathbf{x}))$ expanded as a polynomial in λ.] It follows that, for $\mathbf{x} \in E_e$, we have

$$\begin{cases} \dot{V}_e = 0 & \text{at } \mathbf{x}_e = \mathbf{0} \ (\text{i.e., } \hat{\mathbf{x}} = \mathbf{x}) \\ \dot{V}_e < 0 & \text{elsewhere.} \end{cases}$$

Thus when $\mathbf{x} \in E_e$, the L_2-norm of the state estimation error $\mathbf{x}_e$ decreases uniformly in time.   □

Note that E_e is nonempty for at least some L. For example, even for $L = 0$ (i.e., no measurement feedback at all) the region near the line $x_3 = \sigma$, $x_2 = 0$ has all negative eigenvalues.

Unfortunately, it does not appear (for the present parameter values) to be possible to select linear estimator feedback L such that the entire absorbing ball E of the state $\mathbf{x}$ (derived in Lemma 1) is contained in the domain E_e inside of which convergence of the estimator is assured (Lemma 3). Weaker conditions which result in an estimator which is sufficient for the present problem are discussed in Sec. IV.

APPENDIX D: NORM INDEPENDENCE OF THE LYAPUNOV EXPONENT

In this appendix, it is shown that, for finite-dimensional systems, the value of the Lyapunov exponent is independent of the norm used in its definition, although the local Lyapunov exponent is not. As the Lyapunov exponent is the time average of the local Lyapunov exponent, this is an interesting and perhaps counterintuitive observation. In addition, when the Euclidean norm is used, a simple physical interpretation may be assigned to the local Lyapunov exponent.

We first note the norm equivalence principle: for any vector norm $\|\mathbf{x}\|$ of a finite-dimensional vector $\mathbf{x}$ satisfying

(1) nonnegativity $\|\mathbf{x}\| \geq 0$ with $\|\mathbf{x}\| = 0 \Leftrightarrow \mathbf{x} = \mathbf{0}$,

(2) homogeneity $\|\alpha \mathbf{x}\| = |\alpha| \cdot \|\mathbf{x}\|$ for all complex scalars α, and

(3) the triangle inequality $\|\mathbf{x} + \mathbf{y}\| \leqslant \|\mathbf{x}\| + \|\mathbf{y}\|$,

the following inequality holds:

$$C_1 \|\mathbf{x}\|_2 \leqslant \|\mathbf{x}\| \leqslant C_2 \|\mathbf{x}\|_2,$$

where $\|\mathbf{x}\|_2$ denotes the Euclidean norm. Note that, as the dimension of the system under consideration increases, the ratio C_2/C_1 also increases, and thus these bounds are not very tight for high-dimensional systems.

Now consider bounds on the expression for λ_∞ (which we denote here by P) as defined with any norm $\|\mathbf{x}\|$ satisfying the above listed properties by a similar expression (which we denote here by Q) defined with the Euclidean norm $\|\mathbf{x}\|_2$. By the norm equivalence principle cited above, it follows that

$$P \triangleq \lim_{T \to \infty} \frac{1}{T} \log \frac{\|\delta\mathbf{x}(T)\|}{\|\delta\mathbf{x}(0)\|}$$

$$\leqslant \lim_{T \to \infty} \frac{1}{T} \log \frac{C_2 \|\delta\mathbf{x}(T)\|_2}{C_1 \|\delta\mathbf{x}(0)\|_2}$$

$$= \lim_{T \to \infty} \frac{1}{T} \log \frac{\|\delta\mathbf{x}(T)\|_2}{\|\delta\mathbf{x}(0)\|_2} \triangleq Q.$$

By a similar calculation, it follows that

$$P = \lim_{T \to \infty} \frac{1}{T} \log \frac{\|\delta\mathbf{x}(T)\|}{\|\delta\mathbf{x}(0)\|}$$

$$\geqslant \lim_{T \to \infty} \frac{1}{T} \log \frac{C_1}{C_2} \frac{\|\delta\mathbf{x}(T)\|_2}{\|\delta\mathbf{x}(0)\|_2}.$$

$$= \lim_{T \to \infty} \frac{1}{T} \log \frac{\|\delta\mathbf{x}(T)\|_2}{\|\delta\mathbf{x}(0)\|_2} = Q.$$

We have arrived at the inequality $Q \leqslant P \leqslant Q$, and thus it follows that $P = Q$, i.e., the Lyapunov exponent computed with any norm satisfying the above listed properties is identical to that computed with the Euclidean norm in a finite-dimensional system. Note that the proof utilizes the $T \to \infty$ limit and thus a similar proof does not follow for the local Lyapunov exponent.

In the special case in which we use the Euclidean norm in its definition, we can assign the local Lyapunov exponent a simple physical interpretation:

$$\lambda_\epsilon(\mathbf{x}(t)) = \lim_{T \to 0} \frac{1}{T} \log \frac{\|\delta\mathbf{x}(t+T)\|_2}{\|\delta\mathbf{x}(t)\|_2}$$

$$= \lim_{T \to 0} \frac{1}{2T} \log \frac{(\delta\mathbf{x}(t) + T\delta\dot{\mathbf{x}}(t))^*(\delta\mathbf{x}(t) + T\delta\dot{\mathbf{x}}(t))}{\delta\mathbf{x}(t)^* \delta\mathbf{x}(t)}$$

$$= \lim_{T \to 0} \frac{1}{2T} \log \frac{\delta\mathbf{x}(t)^* \delta\mathbf{x}(t) + 2T\delta\dot{\mathbf{x}}(t)^* \delta\mathbf{x}(t) + T^2 \delta\dot{\mathbf{x}}(t)^* \delta\dot{\mathbf{x}}(t)}{\delta\mathbf{x}(t)^* \delta\mathbf{x}(t)}$$

$$= \frac{\delta\dot{\mathbf{x}}(t)^* \delta\mathbf{x}(t)}{\delta\mathbf{x}(t)^* \delta\mathbf{x}(t)}$$

$$= \frac{\|\delta\dot{\mathbf{x}}(t)\|_2}{\|\delta\mathbf{x}(t)\|_2} \cos \sphericalangle (\delta\dot{\mathbf{x}}(t), \delta\mathbf{x}(t)).$$

The final expression is simply the ratio of the magnitudes of $\delta\dot{\mathbf{x}}(t)$ and $\delta\mathbf{x}(t)$ times the cosine of the angle between them. Naturally, if the cosine of this angle is positive, the magnitude of the perturbation in the Euclidean norm is increasing, and if it is negative, the magnitude of the perturbation is decreasing.

[1] E. N. Lorenz, ''Deterministic nonperiodic flow,'' J. Atmos. Sci. **20**, 130–141 (1963).

[2] B. Saltzman, ''Finite amplitude free convection as an initial value problem—I,'' J. Atmos. Sci. **19**, 329–341 (1962).

[3] Y. Z. Wang, J. Singer, and H. H. Bau, ''Controlling chaos in a thermal convection loop,'' J. Fluid Mech. **237**, 479–498 (1992).

[4] J. Gleick, *Chaos: Making a New Science* (Viking, New York, 1987).

[5] J. A. Yorke, and E. E. Yorke, ''Chaotic behavior and fluid dynamics,'' in *Hydrodynamic Stability and the Transition to Turbulence*, edited by H. L. Swinney and J. Gollub, Topics in Applied Physics, Vol. 45 (Springer, New York, 1982), pp. 77–95.

[6] M. Gorman, P. J. Widmann, and K. A. Robins, ''Nonlinear dynamics of a convection loop: A quantitative comparison of experiment with theory,'' Physica 19D, 255–267 (1986).

[7] P. J. Widmann, M. Gorman, and K. A. Robins, ''Nonlinear dynamics of a convection loop ii. Chaos in laminar and turbulent flows,'' Physica D **36**, 157–166 (1989).

[8] J. E. Hart, ''A new analysis of the closed loop thermosyphon,'' Int. J. Heat Mass Transf. **27**, 125–136 (1984).

[9] C. Sparrow, *The Lorenz Equations: Bifurcations, Chaos, and Strange Attractors* (Springer, New York, 1982).

[10] E. N. Lorenz, *The Essence of Chaos* (University of Washington Press, Seattle, 1993).

[11] T. Shinbrot, C. Grebogi, E. Ott, and J. A. Yorke, ''Using small perturbations to control chaos,'' Nature (London) **363**, 411–417 (1993).

[12] J. M. Nese, ''Quantifying local predictability in phase space,'' Physica D **35**, 237–250 (1989).

[13] B. Eckhardt, and D. Yau, ''Local Lyapunov exponents in chaotic systems,'' Physica D **65**, 100–108 (1989).

[14] B. F. Farrell, and P. J. Ioannou, ''Generalized stability theory. Part II: Nonautonomous operators,'' J. Atmos. Sci. **53**, 2041–2053 (1996).

[15] T. L. Vincent, ''Control using chaos,'' IEEE Control Syst. Mag. **17**, 65–76 (1997).

[16] P. K. Yuen, and H. H. Bau, ''Optimal and adaptive control of chaotic convection—Theory and experiments,'' Phys. Fluids (submitted).

[17] T. L. Vincent, and J. Yu, ''Control of a chaotic system,'' Dynamics and Control **1**, 35–52 (1991).

[18] H. H. Bau and Y. Z. Wang, ''Chaos: A heat transfer perspective,'' in *Annual Review of Heat Transfer*, edited by C. L. Tien, Vol. 4, pp. 1–50 (1991).

[19] H. Wang and E. H. Abed, ''Bifurcation control of chaotic dynamical systems,'' University of Maryland Institute for Systems Research, Technical Research Report 92–67 (1992).

[20] C.-J. Wan and D. S. Bernstein, ''Nonlinear feedback control with global stabilization,'' Dynamics and Control **5**, 321–346 (1995).

[21] P. K. Yuen and H. H. Bau, ''Rendering a subcritical Hopf bifurcation supercritical,'' J. Fluid Mech. **317**, 91–109 (1996).

[22] T. R. Bewley and S. Liu, ''Optimal and robust control and estimation of linear paths to transition,'' J. Fluid Mech. **365**, 305–349 (1998).

[23] A. J. Laub, ''Invariant subspace methods for the numerical solution of Riccati equations,'' in *The Riccati Equation*, edited by Bittaini, Laub, and Willems (Springer, New York, 1991), pp. 163–196.

[24] J. C. Doyle, K. Glover, P. P. Khargonekar, and B. A. Francis, ''State-space solutions to standard $\mathcal{H}_2$ and $\mathcal{H}_\infty$ control problems,'' IEEE Trans. Autom. Control. **34**, 831–847 (1989).

[25] F. L. Lewis and V. L. Syrmos, *Optimal Control* (Wiley, New York, 1995).

[26] M. Green and D. J. N. Limebeer, *Linear Robust Control* (Prentice-Hall, New York, 1995).

[27] S. Skogestad and I. Postlethwaite, *Multivariable Feedback Control* (Wiley, New York, 1996).

[28] J. Malmborg, B. Bernhardsson, and K. J. Åström, ''A stabilizing switching scheme for multi controller systems,'' Proceedings of the 13th World Congress of IFAC, F, San Francisco, pp. 229–234 (1996).

[29] K. Ezal, Z. Pan, and P. V. Kokotović, ''Locally optimal backstepping design,'' Proceedings of the 36th IEEE Conference on Decision and Control, San Diego (1997).

[30] M. Janković, R. Sepulchre, and P. V. Kokotović, ''Constructive Lyapunov stabilization of nonlinear cascade systems,'' IEEE Trans. Autom. Control. **41**, 1723–1735 (1996).

[31] M. Janković, private communication (1997).

[32] P. K. Kokotović, ''The joy of feedback: Nonlinear and adaptive,'' IEEE Control Syst. Mag. **12**, 7–17 (1992).

[33] P. Moin and T. R. Bewley, ''Application of control theory to turbulence,'' Twelfth Australasian Fluid Mechanics Conference, December 10–15, 1995, Sydney, pp. 109–117.

[34] S. K. Robinson, ''Coherent motions in the turbulent boundary layer,'' Annu. Rev. Fluid Mech. **23**, 601–639 (1991).

[35] J. Jeong, F. Hussain, W. Schoppa, and J. Kim, ''Coherent structures near the wall in a turbulent channel flow,'' J. Fluid Mech. **332**, 185–214 (1997).

[36] T. R. Bewley, P. Moin, and R. Temam, ''DNS-based predictive control of turbulence: an optimal target for feedback algorithms,'' J. Fluid Mech. (submitted).

[37] P. Holmes, J. L. Lumley, and G. Berkooz, *Turbulence, Coherent Structures, Dynamical Systems and Symmetry* (Cambridge University Press, Cambridge, 1996).

[38] T. R. Bewley, P. Moin, and R. Temam, ''A method for optimizing feedback control rules for wall-bounded turbulent flows based on control theory,'' Proceedings of the ASME Fluids Engineering Summer Meeting, ASME FED Vol. 237, p. 279–285 (1996).

[39] T. R. Bewley, R. Temam, and M. Ziane, ''A general framework for robust control in fluid mechanics,'' Physica D (submitted).

[40] C. Lee, J. Kim, D. Babcock, and R. Goodman, ''Application of neural network to turbulence control for drag reduction,'' Phys. Fluids **9**, 1740–1747 (1997).

[41] A. van der Schaft, L_2-*Gain and Passivity Techniques in Nonlinear Control* (Springer, New York, 1996).

[42] A. Isidori, *Nonlinear Control Systems* (Springer, New York, 1995).

[43] D. Graham and D. McRuer, *Analysis of Nonlinear Control Systems* (Wiley, New York, 1961).